DEVELOPMENT AND USE OF A *G. MELLONELLA* INFECTION MODEL TO DISCOVER NOVEL VIRULENCE MUTANTS IN *B. ANTHRACIS*.

by

JACOB ADAM MALMQUIST

Bachelor of Science, 2016
Texas Christian University
Fort Worth, Texas

Submitted to the Graduate Faculty of the
College of Science and Engineering
Texas Christian University
in partial fulfillment of the requirements
for the degree of

Master of Science

May 2018

DEVELOPMENT AND USE OF A *G. MELLONELLA* INFECTION MODEL TO DISCOVER NOVEL VIRULENCE MUTANTS IN *B. ANTHRACIS.*

by

Jacob Malmquist

Thesis approved:

Major Professor

For The College of Science and Engineering

ACKNOWLEDGEMENTS

Over the past six years, my knowledge of science, discovery, and perseverance has been shaped by the incredible faculty of the TCU Biology Department. First off, I want to thank Dr. Shauna McGillivray for guiding me through this project. She provided me with the necessary assistance but also allowed me to develop my own problem-solving skills which are essential to becoming an independent scientist. These skills will also be paramount in my future endeavors. I would also like to thank the rest of my advisory committee, Drs. Giri Akkaraju and Meredith Curtis, for their wisdom and inspiration to being constantly curious. Additionally, this project required significant help from Dr. Dean Williams for his expertise in DNA sequencing. On the financial side, this project could not be completed without the support of the Adkins fund.

I would also like to thank my incredible support system for bearing with me throughout the last two years. Madison Garrett, you have been so understanding with my constant need to stop at the lab to start cultures or "check my worms" as well as my constant attention to Microsoft Word and my data during this spring semester. To my family, you have been accepting of my need to be in the lab and miss out on family time.

Overall, I have loved being in this graduated program. I have become a more capable scientist with the skills necessary to operate independently in the lab, delve through the literature, and make conclusions. Without the guidance of these special mentors and so many more, I would not be as prepared and ready to succeed in the future.

TABLE OF CONTENTS

LIST OF FIGURES

LIST OF TABLES

INTRODUCTION

Bacillus anthracis is a gram-positive, endospore forming bacterium that is the causative agent for the human disease, anthrax. While this bacterium is frequently found in soil, most human cases arise after contact with infected animals (Watson & Keir, 1994). Anthrax is initiated when endospores are transmitted to humans through cutaneous wounds, ingestion of infected food sources, or inhalation. These spores are not metabolically active, but they are exceedingly resistant to many physical and chemical control mechanisms (drying, heat, ultraviolet radiation) (Dixon, Meselson, Guillemin, & Hanna, 1999). When these spores are transmitted to humans, this provides the nutrient rich environment needed for the spores to germinate into the metabolically active, vegetative form, thus establishing an infection. Depending on the location of infection, Anthrax has varying prognoses. The most serious form of infection, inhalational anthrax, causes a systemic infection, usually leading to death (Dixon et al., 1999). Because of the ease of transmission and severity of disease, the National Institute of Allergy and Infectious Diseases classifies *B. anthracis* as a Category A Priority Pathogen indicating that it poses the highest risk to national security and public health. Historically, *B. anthracis* has been used as a bioterror weapon, most notably in 2001, when endospores were released in the US mail, resulting in 18 confirmed cases of anthrax (11 inhalational, 7 cutaneous), and 5 deaths (Harris, 2002; Jernigan et al., 2002).

Two important contributors to the virulence of *B. anthracis* include the anthrax toxins lethal toxin and edema toxin, which are encoded on the pX01 plasmid, and the capsule, which is encoded on the pX02 plasmid. These contribute to the associated symptoms of anthrax and help the bacterium evade the immune system when establishing an infection (Dixon et al., 1999). The virulence factors encoded on the pX01 and pX02 plasmids have been well characterized and are critical in establishing disease. However, less is known about chromosomally-encoded proteins

and the role they may play in the pathogenesis of anthrax. After genome sequencing of the Ames strain (pX01^{+}, pX02^{-}) of *B. anthracis*, many putative virulence factors were identified, including haemolysins, phospholipases, and siderophores (Read et al., 2003). Homologs of these proteins have been observed to aid in evasion of the immune system and enhance damage to the host in other pathogens such as *Listeria monocytogenes* and *Yersinia pestis* (Read et al., 2003). This leads to the question of whether chromosomally-encoded proteins are contributing to the pathogenesis of anthrax.

In order to investigate the contribution of chromosomal genes in anthrax disease, our lab previously constructed a 5,000 transposon mutant library designed to identify potential chromosomal virulence targets (McGillivray et al., 2009). Transposon mutants were narrowed down by screening for attenuated virulence-associated phenotypes in 3 independent screens assaying for proteolytic activity, hemolytic activity and virulence in *Caenorhabditis elegans* (Franks et al., 2014; McGillivray et al., 2009). Hemolytic and proteolytic activity play an important role in bacterial pathogenesis. Hemolysis aids in the sequestering of iron, a key nutrient for biochemical processes, and proteolytic activity aids the pathogen in invasion of tissues and evasion of host antimicrobial proteins (Doherty, 2007). At the conclusion of these initial screens, 44 mutants had an altered phenotype in at least one of these screens. Two of these mutants, the *clpX*, which functions as part of the ClpXP protease, and *yceGH,* which is important in resistance to reactive oxygen species, were further characterized and implicated in virulence in animal models of anthrax (Franks et al., 2014; McGillivray et al., 2009). This demonstrates that this method of identifying novel virulence genes through randomly generated mutations is successful and that these screens can identify novel virulence factors.

In order to further narrow down these 44 transposon mutants, Madison Rogan, a previous undergraduate student, exposed these mutants to hydrogen peroxide (H_2O_2). H_2O_2 belongs to a

class of compounds called reactive oxygen species (ROS). ROS are created by NADPH oxidase in the phagolysosome and cell membrane of host cells and they have antimicrobial effects by inducing oxidative damage to bacterial structures (Dan Dunn, Alvarez, Zhang, & Soldati, 2015). If a pathogen does not have a way to evade or detoxify ROS, then damage to DNA and membranes will cause bacterial death. Therefore, resistance mechanisms to H_2O_2 are an immune evasion strategy that facilitates the survival of many bacterial pathogens. Of the 44 selected mutants, 12 had increased susceptibility to H_2O_2 in high-throughput minimum inhibitory concentration (MIC) assays, as evidenced by decreased growth when exposed to H_2O_2 in comparison to the parental wild-type strain (Rogan, unpublished).

Additionally, 5 mutants were identified in screens performed by previous undergraduate students, Julio Manceras and Mariah Green, as being unable to acquire iron from hemoglobin. The functional aspect of hemoglobin, heme, is an iron-porphyrin molecule found in erythrocytes which binds oxygen and transports it to metabolically active tissues (Andrews, 2000; Balderas, Nobles, Honsa, Alicki, & Maresso, 2012; Fedhila et al., 2010). In *B. anthracis*, iron has been associated with proper functioning of electron transfer proteins and superoxide dismutase enzymes, thus showing the importance of this metal (Tu et al., 2012). In order to establish an infection, wild type *B. anthracis* strips iron from hemoglobin and uses it to sustain life in the host (Balderas et al., 2012; Cendrowski, MacArthur, & Hanna, 2004). Identification of *B. anthracis* genes involved in iron acquisition provides insight into how chromosomal genes may act as virulence factors.

Ultimately, identification of potential virulence genes requires not only *in vitro* assays, but also a means to test potential phenotypes *in vivo*. Traditional infection models use the mouse, *Mus musculus,* but logistical, financial, and ethical concerns limit the scope of this mode of *in vivo* testing. Due to these concerns, there has been a push to develop a new invertebrate model

for infection studies since they are easy to work with and do not have the regulation and resource demands of a vertebrate model. A common laboratory invertebrate, *C. elegans*, has been used as a potential *in vivo* model. This nematode possesses immune signaling pathways (e.g. MAP Kinase) as well as antimicrobial peptides, reactive oxygen species, and detoxifying agents (e.g. metallothioneins) (Chávez, Mohri-Shiomi, & Garsin, 2009; Gravato-Nobre & Hodgkin, 2005; Kato et al., 2002). Despite these positive characteristics, *C. elegans,* as a bacterial *in vivo* model, possesses some limitations. In previous studies where *C. elegans* has been used as a model for *B. anthracis* infection, additional stresses needed to be placed on the worms in order for them to be susceptible to infection, which made this a highly manipulated model (Franks et al., 2014). Additionally, *C. elegans* cannot be incubated at 37°C, the optimal infection temperature for bacterial pathogens, and the only mode of infection is through ingestion, which can lead to uneven exposure to pathogen (Franks et al., 2014; Gravato-Nobre & Hodgkin, 2005; Kho et al., 2011; Laaberki & Dworkin, 2008). These constraints can lead to inconsistencies in reproducing infection results, demonstrating a need for a better invertebrate *in vivo* model.

Another potential invertebrate *in vivo* models are insects. In general, insects boast an immune system which mimics the vertebrate innate immune system (Salzet, 2018). Their cuticle is made up of a waxy outer layer which contains antimicrobial lipids, fatty acids, and sterols (Clarkson & Charnley, 1996). This creates a distinct barrier that prevents infection much like vertebrate skin. When the cuticle is breached the haemolymph, analogous to blood, contains antimicrobial peptides, reactive oxygen species, and cellular elements, named haemocytes, which restrict the pathogen's invasion of host tissue and also kills the pathogen (Bolouri Moghaddam et al., 2016; Morton, Dunphy, & Chadwick, 1987; Vilmos & Kurucz, 1998). At least six different classes of haemocytes are present in Lepidoptera which have many functions--phagocytosis, nodulation, encapsulation, melanisation and clotting (Boman & Hultmark, 1987; Kavanagh &

Reeves, 2004). One Lepidoptera species, *Galleria mellonella*, has garnered substantial evidence as being a reliable *in vivo* model for infection studies. Previous studies have shown its susceptibility to *Pseudomonas aeruginosa*, *Acinetobacter baumannii*, *Staphylococcus aureus*, *Cryptococcus neoformans*, and *Candida albicans* virulence (Cotter, Doyle, & Kavanagh, 2000; Mylonakis et al., 2005; Peleg et al., 2009; Purves, Cockayne, Moody, & Morrissey, 2010). One study attempted to use oral infection of *G. mellonella* with *B. anthracis* to discern virulence but was unsuccessful (Fedhila et al., 2010). Therefore, further investigation into validating *G. mellonella* as a suitable animal model for *B. anthracis* infection studies is needed as this would be an efficient, cost-effective, and ethically sound way to assess potential virulence mutants.

The goal of this study is two-fold. Initially, I would like to validate the use of the greater wax moth larvae, *G. mellonella*, as an animal model to study virulence in *B. anthracis.* To do this, I will assess mortality of *G. mellonella* after injection with previously identified *B. anthracis* virulence mutants. Secondly, I would like to further investigate the transposon mutants found to be sensitive to ROS and those unable to acquire iron from hemoglobin. After confirming their *in vitro* phenotype, I would like to further evaluate them in *G. mellonella* for an *in vivo* phenotype. Overall, this study will add evidence to determine the usefulness of *G. mellonella* as an infection model and possibly identify novel chromosomally-encoded virulence factors for *B. anthracis*, potentially prompting a change in methodology for *in vivo* infection studies.

MATERIALS AND METHODS

Bacterial strains and growth conditions. Unless specifically stated, *Bacillus anthracis* Sterne strain (pX01^{+}, pX02^{-}) was cultured in Brain-Heart Infusion (BHI) media (Hardy Diagnostics) at 37°C under aerobic conditions. Media containing antibiotic was used at the following concentrations: *E. coli*: erythromycin 500μg/ml (Erm500), chloramphenicol 50μg/ml (Cm50); *B. anthracis*: erythromycin 5μg/ml (Erm5), chloramphenicol 3μg/ml (Cm3), and kanamycin 50μg/ml (Kan50).

Transposon library and mutant construction. The *B. anthracis* transposon mutant library as well as *ΔclpX*, and *ΔyceGH* mutants of *B. anthracis* were previously constructed (Franks et al., 2014; McGillivray et al., 2009). *ywlE, mntA, hrtA, bNOS, purH*, and *mprF* insertional mutants (IM) were constructed using the temperature sensitive pHY304 plasmid. To create each IM, a *Ywle* 195-bp amplicon, a *MntA* 379-bp amplicon, a *HrtA* 363-bp amplicon, a *bNOS* 315-bp amplicon, a *purH* 367-bp amplicon, and a *mprF* 417-bp amplicon were created via PCR using each gene's respective forward and reverse primers listed in Table 1. The *MntA*, *bNOS*, *purH,* and *mprF* amplicons were each digested with *Xho1* and *HindIII* and ligated into the temperature sensitive plasmid pHY304. The *HrtA* amplicon was digested with *Ecor1* and *Xho1* and also ligated into pHY304. The *Ywle* amplicon was digested with Xbal and Ecor1 and ligated into pHY304. Restriction enzymes and ligases were obtained from New England Biolabs. Newly constructed plasmids were chemically transformed into a commercially available MC1061 *E. coli* strain (Lucigen), plated under Erm500 selection, and incubated at 30°C for selection. Plasmids were then extracted via miniprep (IBI Scientific) and chemically transformed into methylation deficient GM2163 *E. coli* using electroporation, plated on Erm500 selection, and incubated at 30°C for 48 hours. GM2163 grown plasmids were then extracted, chemically

transformed into electrocompetent *B. anthracis*, plated under Erm5 selection, and incubated at 30°C for 48 hours. *B.anthracis* containing the insertional mutant plasmid were then passed three times at 37°C, plated under Erm5 selection, and incubated overnight at 37°C. Confirmation of insertional mutants involved a PCR using inserted plasmid (pHY304) specific primer and a genomic primer to a region downstream of each insertion point. All primers are listed in Table1.

Table 1. List of primers for insertional mutagenesis

Primer Name	Primer Sequence
MntA Fwd	5'- acagtctcgagAACCCGCATGAATATGATCCACTAC -3'
MntA Rev	5'- gactaagcttCGTTTCTCCTCAGGGATTTGATG -3'
MntA Confirm Rev	5'- AGGTAATGGGATTTGGGAAGGTG -3'
HrtA Fwd	5- acgtctcgagTGCAATGCAACCGACAGG -3'
HrtA Rev	5- tacgGAATTCGCACGCTTATCGCCATCGA -3'
HrtA Confirm Rev	5'- AACGACACCTACTCCAAGAGC -3'
bNOS Fwd	5'- acagtctcgagACAGAAATGGGAGTGACTGGTG -3'
bNOS Rev	5'- gactaagcttGATCCGCTAAGTTACGCGCC -3'
bNOS Confirm Rev	5'- CACGACCACAAGCAGCTT -3'
purH Fwd	5'- acagtctcgagAAAGAGAACGGTGAAGTAGCAGAG -3'
purH Rev	5'- gactaagcttCATGAATATCCGTACCTACTCCAACA -3'
purH Confirm Rev	5'- GCTTGCGCTTGTCGCTTT -3'
Ywle Fwd	5'- ACTGTATCTAGAGAGGCGTTACTTCGTCATCATG -3'
Ywle Rev	5'- TACAGTGAATTCGATCCGCCAAATGGGTCTG -3'
Ywle Confirm Rev	5'- GATCCGCCAAATGGGTCTG -3'
Mprf Fwd	5'- ACGTCTCGAGGAAGCAAGCGGAAGGACAAG -3'
Mprf Rev	5'- TACGAAGCTTGTTGTTTCTAATGCAGGCGCA -3'
Mprf Confirm Rev	5'- GTAAGGCGTGTGCTCTGTTT -3'
pHY304 Fwd	5'- ACGACTCACTATAGGGCGAATTGG -3'
pHY304 Rev	5'- GCGGATAACAATTTCACACAGG -3'

Confirmation of functional phenotype. To determine if the constructed mutants demonstrated a comparable phenotype to the literature's description, a variety of assays were performed as described below.

MntA IM ROS: Wild Type (WT) and MntA IM *B. anthracis* strains were grown overnight in BHI and Erm5 respectively generating a stationary phase culture. The stationary phase culture was diluted in BHI to a final concentration of 1:50 in 0.005% H_2O_2 in a total volume of 200µl. The culture was then incubated in a sterile 96-well plate at 37°C for 24 hours. Optical density (OD) was read at a wavelength of 600 nm to quantify bacterial growth.

HrtA IM temperature: WT and HrtA IM *B. anthracis* strains were grown overnight in BHI and Erm5, respectively. The next day, fresh BHI was inoculated at a 1:20 dilution with overnight cultures grown and bacteria were grown until early log phase (OD 0.4). Log phase cultures were then diluted 1:100 and grown in fresh BHI at either 37°C or 44°C. Growth was monitored and the OD was measured every hour for 6 hours.

HrtA IM ROS: Wild Type (WT) and HrtA IM *B. anthracis* strains were grown overnight in BHI and Erm5, respectively. Overnight cultures were diluted 1:20 and then grown at 37°C under aerobic conditions until early log phase (OD 0.4). Log phase cultures were diluted 1:20 in BHI containing 0% or 0.0025% H_2O_2. Culture was incubated in sterile 96 well plate at 37°C and grown for 24 hours with OD readings at indicated times.

bNOS IM: Wild Type (WT) and bNOS IM *B. anthracis* strains were grown overnight in BHI and Erm5 respectively generating a stationary phase culture. The stationary phase culture was diluted in BHI to a final concentration of 1:50 in 0.005% H_2O_2 in a total volume of 200µl of 1:50 final bacterial concentration. The culture was incubated in sterile 96-well plate at 37°C for 8 hours. Optical density (OD) was read at a wavelength of 600nm to quantify bacterial growth.

purH IM: R-minimal media was made using 0.2% Casamino acids (Bacto), 1mg thiamine hydrochloride (TCI), 2500mg glucose (Sigma), 7.4mg $CaCl_2$-$2H_2O$ (Sigma), 9.9mg $MgSO_4$ -H_2O (Sigma), 0.9mg $MnSO_4$ H_2O (Sigma), 3,000mg K_2HPO_4, (Sigma), 8,000mg $NaHCO_3$ (Sigma), 1.4mg uracil (Acros Organic), 2.1mg adenine sulfate (Acros Organic) per liter of milliQ water (Ristroph & Ivins, 1983; Thorne, Molnar, & Strange, 1960). WT and purH IM were incubated overnight in BHI and Erm5, respectively. Overnight cultures were washed and resuspended in PBS then diluted in R-minimal media and fresh BHI at a 1:15 dilution. Cultures were incubated at 37°C under aerobic conditions. OD was determined after 24 hours to quantify bacterial growth.

Reactive oxygen species (ROS) assays. *B. anthracis* transposon mutants were grown overnight. Stationary phase cultures were exposed to ROS (Hydrogen Peroxide: 0.01-0.02%, Sodium Hypochlorite: 0.12%) at a final dilution of 1:50 in 200µl BHI. Assay was incubated at 37°C in 96 well plate. Starting cultures were plated and colonies counted to confirm equivalent colony forming units (cfu) per ml.

Iron acquisition from hemoglobin. To make chelated RPMI (cRPMI), 3g of Chelex 100 sodium beads (Sigma) were used per 100ml RPMI. Mixture was incubated for one hour to remove free iron, and then sterilely filtered to make cRPMI. RPMI and cRPMI were then supplemented with 50µl of 200µM stock lyophilized bovine hemoglobin (Hb) (Sigma) yielding a final concentration of 10µM. Hemoglobin stock (200µM) did not have to be sterilely filtered. 10µL of each overnight culture, grown in Kan50, was used to inoculate 990µL of RPMI+Hb, cRPMI, and cRPMI+Hb, cultures were incubated at 37°C under shaken, aerobic conditions for 48 hours. Growth was measured via optical density.

Y-linker PCR. Protocol was adapted from Kwon and Ricke 2000 (Kwon & Ricke, 2000). Primers used are listed in Table 2. 11.6µl of Linker 2 stock (100µM) was diluted with 28.4µl of water yielding 40µl of 350ng/µl. 18µl of linker 2 dilution was phosphorylated with PNK (NEB) in T4 ligase buffer at 37°C for one hour. Then, PNK was heat denatured at 65°C for 20 minutes. 10.6µl of Linker 1 stock (100µM) was diluted with 28.4µl of water yielding 40µl of 350ng/µl. 18µl of diluted Linker 1 was annealed to phosphorylated Linker 2 by heating primers at 95°C for 5 minutes and slowly cooling to room temperature. Annealing was done via boiling water for five minutes and then taking beaker off the heat to cool. To room temperature. This process yielded ~200ng/µl of a created Y-linker. 5µg of phenol/chloroform extracted transposon mutant genomic DNA was digested with *NlaIII* (NEB). 200 ng of digested DNA was then ligated to 1µg of Y-linker with T4 ligase (NEB), heat denatured, and used as a template for PCR. Himar 1-2 long, a transposon specific primer, and a Y-linker specific primer were used to amplify a fragment that contained a transposon region, genomic region, and Y-linker region. The PCR product was then sequenced and the results were BLASTed against the *B. anthracis* genome.

Table 2. List of primers used in Y-linker protocol

Primer Name	Primer Sequence
Linker 1	5'- TTTCTGCTCGAATTCAAGCTTCTAACGATGTAC GGGGACACATG -3'
Linker 2	5'- TGTCCCCGTACATCGTTAGAACTACTCGTACCA TCCACAT -3'
Y-linker primer	5'- CTGCTCGAATTCAAGCTTCT -3'
Himar 1-2 long	5'- GGGAATCATTTGAAGGTTGGTACT -3'

***Galleria mellonella* survival assay.** *G. mellonella* were obtained from Rainbow Mealworms (www.rainbowmealworms.net). Larvae weighing 190-200mg were placed into groups of ten for injection. Larvae were kept at 4°C prior to injection to reduce movement. *B. anthracis* strains were grown overnight, diluted 1:20, and grown to early log phase (OD 0.4) in BHI. Once OD 0.4 was reached, bacteria were washed and suspended in PBS at a 1:2 dilution. Larvae were injected with 10µl of 1:2 diluted bacteria (approximately $8x10^4$ cfu/larvae) and starting amounts were confirmed through colony counts of original cultures. After injection, larvae were observed at room temperature to ensure they recovered from injection and were transferred to an incubator at 37°C. Surviving larvae were counted at 24, 48, and 72-hours post injection.

***Galleria mellonella* competition assay.** Larvae weighing 170-230mg were kept at 4°C prior to injection. *B. anthracis* strains were grown overnight in antibiotic selective media at 37°C under aerobic conditions. Overnight cultures were used to start day cultures in BHI media. Once the day cultures reached early log phase (OD 0.4), log phase cultures were washed and resuspended in PBS. Mutant strains are then mixed with wild-type *B. anthracis* at a 50/50 ratio then plated on BHI and antibiotic media (Erm5 and Kan50, depending on the mutant) to ensure even mixture.

As a control, a 1:40 dilution of the mixed culture was homogenized by bead-beating with 1mm ceramic beads (4.5m/sec for 2 cycles of 45sec) and plated on BHI and antibiotic selective media. 10µl of undiluted mixed culture was then injected into posterior of larvae. After injection, larvae were observed at room temperature to ensure they recovered from injection and were transferred to an incubator at 37°C for 6 hours. After incubation, larvae were homogenized with 400µl PBS by bead beating (4.5m/sec for 2 cycles of 45secs) with 1mm ceramic beads and where plated on both BHI and antibiotic selective media to determine the percent of each strain contributing to the infection. Recovery of mutant was determined by counting the number of colonies grown on the antibiotic plate. Recovery of wild-type was determined by subtracting the number of colonies grown on the antibiotic plate from the number of colonies grown on the plain BHI plate. Percent recovery of wild-type was calculated by dividing the number of wild-type colonies by the number of colonies counted on the plain BHI plate and multiplying by 100. Percent recovery of mutant was calculated by dividing the number of mutant colonies by the number of colonies counted on the plain BHI plate and multiplying by 100.

Statistics and Analysis. Graph pad prism was used for all analysis. Student's T test and One-way ANOVA were used for all *in vitro* analysis. For *in vivo* assessment, the Kaplan-Meier survival analysis was used to generate p-value. To correct for multiple comparison, level of statistical significance of α=0.05 divided by the number of treatment groups.

RESULTS

Attenuated virulence can be detected by *Galleria mellonella.*

Our first goal of this study was to validate *G. mellonella* as an infection model for *B. anthracis* Sterne, an unencapsulated *B. anthracis* strain that lacks the pX02 plasmid and is safe to use in a BSL-2 facility. To do this, we had to determine not only that *G. mellonella* can be infected with wild-type *B. anthracis* Sterne but also that it can differentiate between virulent and avirulent strains. *G. mellonella* larvae were ordered from an online bait shop and separated into treatment groups of 10 larvae weighing 190-220mg each (Fig. 1A). Standardizing weight is important to ensure that mortality is due to innate differences in treatment conditions (i.e. bacterial strains) as opposed to significant differences in larval weight. *B. anthracis* cultures were grown to log phase (OD 0.4), washed in phosphate buffered saline (PBS), and diluted 1:2. Each larvae was injected with 10µl of this 1:2 dilution yielding ~$8x10^4$ CFU of one bacterial strain or injected with 10µl PBS and incubated at 37°C. Mortality was then monitored over the next 72 hours. One advantage of *G. mellonella*, over other invertebrate models, is the ability to incubate the larvae at 37°C, which is the ideal temperature for bacterial pathogens. Mortality was easy to observe because after death, the larvae turned black (Fig. 1B, black arrow) while the thriving larvae are a cream color (Fig. 1B, red arrow). As expected, uninjected (UI) *G. mellonella* larvae had nominal mortality (Fig. 1C, green line). Injection with PBS increased mortality slightly, although this was not significantly different than the uninjected control (Fig. 1C, red line). Therefore, trauma due to injection does not significantly induce mortality in *G. mellonella*. When injected with wild-type *B. anthracis* Sterne, upwards of 80% mortality was observed (Fig. 1C, black line), thus demonstrating that *B. anthracis* Sterne causes disease in *G. mellonella*. The next step was to determine whether *G. mellonella* could differentiate between the wild-type and an avirulent strain of *B. anthracis* Sterne. Our lab possesses a *ΔpX01* strain of

B. anthracis Sterne, which does not contain the plasmid encoding the anthrax toxins. This mutant is severely attenuated and demonstrates no virulence in mammalian infection models (van Sorge et al., 2008). When injected into *G. mellonella,* the ~20% mortality of *ΔpX01* was comparable to the uninjected and saline injected controls. This is significantly different than that of the wild-type (Fig. 1C, blue line). These results indicate that *G. mellonella* meets the initial requirements of an *in vivo* bacterial infection model: infection and differential survival.

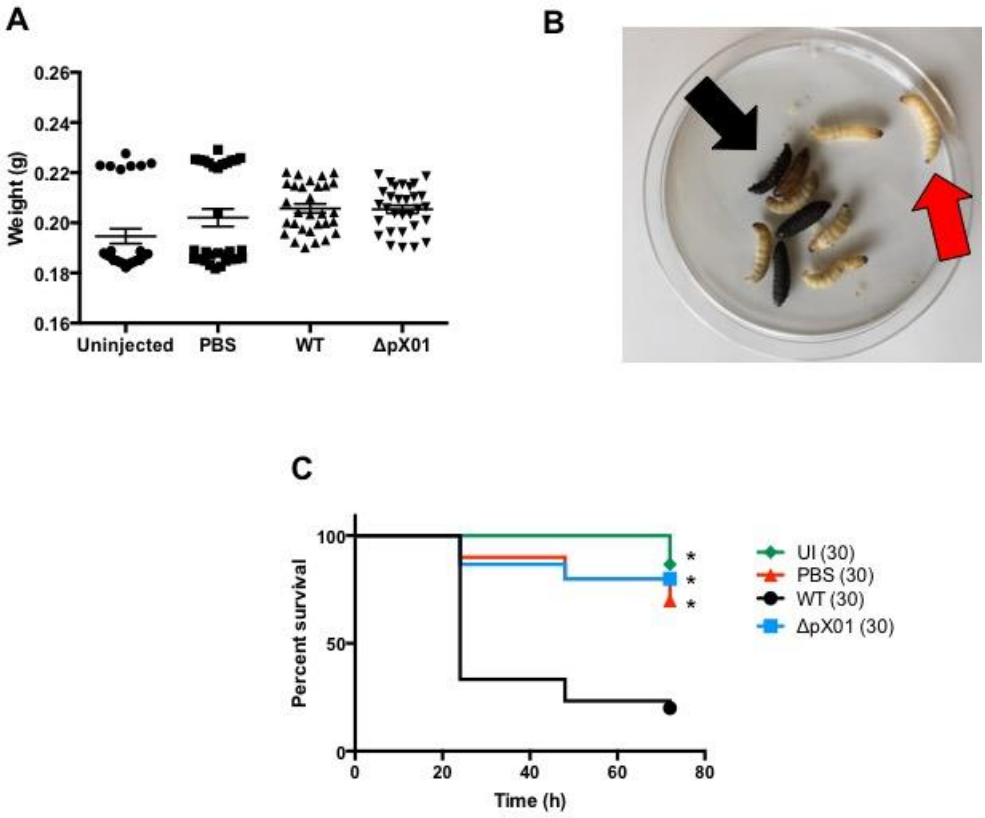

Figure 1. Virulence mutants show attenuated survival in *G. mellonella.* A) Larval weights for each injection group. B) Infected *G. mellonella* with dead larvae (black arrow) and living larvae (red arrow). C) Percent survival of uninjected (UI) larvae, larvae injected with saline (PBS), wild-type *B. anthracis* Sterne (WT), and *ΔpX01* mutant at 24, 48, and 72 hours. Each infection was repeated at least 3 independent times with 10 larvae per condition. Combined results are shown. Total number of larvae for each injection condition are indicated in parenthesis. Significance in comparison to the WT *, $p<0.05$.

Construction and verification of additional known virulence mutants.

While we have shown that *G. mellonella* can respond differently to virulent and avirulent bacteria, we only tested one avirulent mutant, *ΔpX01*, which is extremely attenuated. In order to further validate our model, we wanted to test additional virulence mutants. Our lab already possessed two chromosomal virulence mutants, *ΔclpX* and *ΔyceGH*, that have already been confirmed in a mouse model (Franks et al., 2014; McGillivray et al., 2009). We chose an additional five virulence mutants: *MntA, HrtA, bNOS, purH,* and *mprf* to use for further assessment of our larval model. We chose these mutants because they have all been verified in mammalian infection models, and they possess virulence defects to immune defenses that are likely to exist in *G. mellonella* such as increased sensitivity to ROS and AMPs. Additionally, 4 of these mutants, *ΔclpX, MntA, HrtA,* and *purH* were shown to have a mammalian virulence phenotype in the fully virulent ($pX01^+$, $pX02^+$) *B. anthracis* strain. The specific virulence phenotypes and strains tested are summarized in Table 3.

Table 3. Identity and function of mammalian virulence mutants

Gene	Function	Phenotype	Strain used for in vivo testing (mammalian)	Gene Number	Reference
clpX	Protease	AMP susceptibility	Ames ($pX01^+$, $pX02^+$)	BAS 4369	(McGillivray et al., 2009)
yceGH	Tellurium resistance	ROS and AMP susceptibility	Sterne ($pX01^+$, $pX02^-$)	BAS 3089/3090	(Franks et al., 2014)
MntA	Transporter	ROS susceptibility	Vollum ($pX01^+$, $pX02^+$)	BAS3189	(Gat et al., 2005)
HrtA	Protease	ROS susceptibility and growth deficits	Vollum ($pX01^+$, $pX02^+$)	BAS3660	(Chitlaru et al., 2011)
bNOS	Nitric Oxide sythase	ROS susceptibility	Sterne ($pX01^+$, $pX02^-$)	BAS5299	(Shatalin et al., 2008)
purH	Purine Biosynthesis	Nutritional deficits	Ames ($pX01^+$, $pX02^+$)	BAS0285	(Jenkins et al., 2011)
mprf	Lysyl-phosphatidyl-glycerol synthesis	AMP susceptibility	Sterne ($pX01^+$, $pX02^-$)	BAS1486	(Samant, Hsu, Neyfakh, & Lee, 2009)

We constructed these mutants using insertional mutagenesis. In this technique, the pHY304 plasmid is inserted, via homologous recombination, into a gene of interest. This insertion inactivates this gene, generating a functional knockout (see schematic for the insertional mutant (IM) in Fig. 2A). We confirmed plasmid insertion with PCR using a pHY304 plasmid specific forward primer and a genomic primer downstream of the plasmid insertion site (Fig. 2A, yellow arrows). PCR amplification will only occur with this primer combination if plasmid insertion has occurred in the appropriate location. We successfully generated insertional mutants for *MntA, HrtA, bNOS,* and *purH* with this PCR confirmation (Fig. 2B), however, we were unable to confirm *mprf* insertion using the plasmid specific and genomic primers. Instead, we utilized primers that flanking either side of the *mprf* gene (Fig. 2A, red arrows). This PCR

would only amplify if the plasmid did not insert. If the plasmid inserted, then amplification would not occur since there would be a ~5,000 bp plasmid in the middle of the *mprf* gene. We observed an ~500 bp band in all of the colonies we screened, which corresponded to that of the wild-type (Fig 2C). Therefore, we were unsuccessful in our attempts to create an insertional mutant for *mprf.*

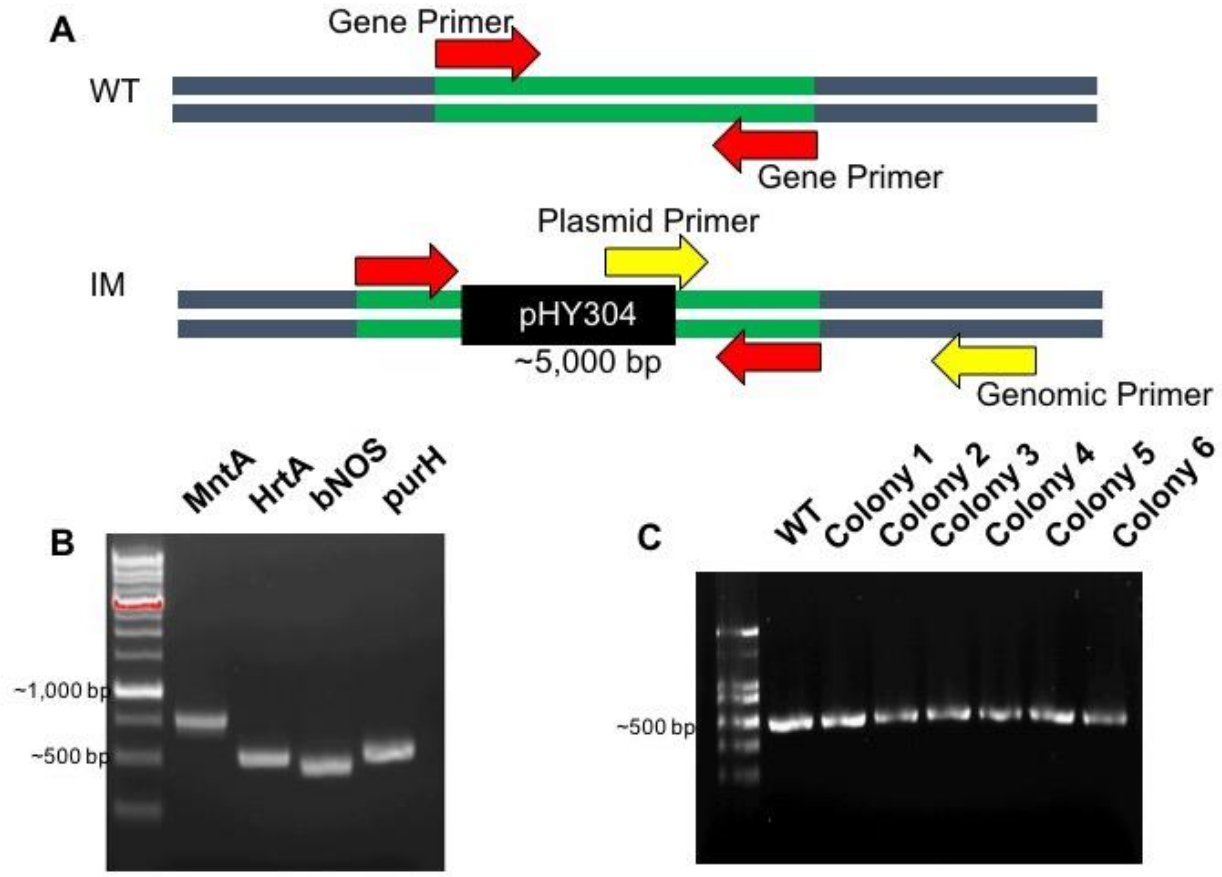

Figure 2. Construction of known mammalian *B. anthracis* virulence mutants. A) Schematic of wild-type (WT) genome and genome of insertional mutant (IM) after mutagenesis. B) Gel of confirmation PCR of insertional mutants using primers represented as yellow arrows in Fig 2A. C) PCR of transitioned *mprf* colonies using primers which flanked the disrupted gene represented by red arrows in Fig 2A.

After constructing these mutants, we wanted to confirm that they exhibited an attenuated virulence phenotype to ensure that the mutant was behaving as predicted. Each mutant was assessed in 1-2 *in vitro* assays based on the published phenotypes for each mutant. The *MntA* gene has been implicated in ROS sensitivity (Gat et al., 2005), so we exposed stationary phase wild-type and *MntA IM* to BHI containing H_2O_2. We found that while growth of wild-type and *MntA IM* was comparable in plain BHI, *MntA IM* was unable to grow when exposed to 0.005% H_2O_2 after 8 or 24 hours of incubation (Fig. 3A). Like *MntA*, *HrtA* also has demonstrated ROS susceptibility as well as growth defects at elevated temperture (Chitlaru et al., 2011). Log phase cultures of wild-type and *HrtA IM* were incubated in plain BHI and BHI containing H_2O_2. Both wild-type and *HrtA IM* grew comparably in BHI, but *HrtA IM* was significantly inhibited in 0.0025% after 8 hours (Fig. 3B, left panel). Despite this initial attenuation in growth, by 24 hours *HrtA IM* growth in 0.0025% H_2O_2 was not significantly different than wild-type (Fig. 3B, right panel). However, we did see that *HrtA IM* growth is significantly attenuated when grown at high temperature (44°C) (Fig. 3C, right panel), which is similar to the published mutant. *purH* has been linked with nutritional deficits and the inability to synthesize purines (Jenkins et al., 2011). Our *purH IM* is unable to grow in purine deficient R-minimal media after 24 hours (Fig. 3F). Loss of *bNOS* has also been linked to increased ROS susceptibility (Shatalin et al., 2008). However, when our *bNOS IM* was exposed to 0.005% H_2O_2, we were unable to see a consistent attenuation in growth. In some assays the mutant was attenuated but not in others leading to a high standard error and no significant difference when compared to the wild-type.

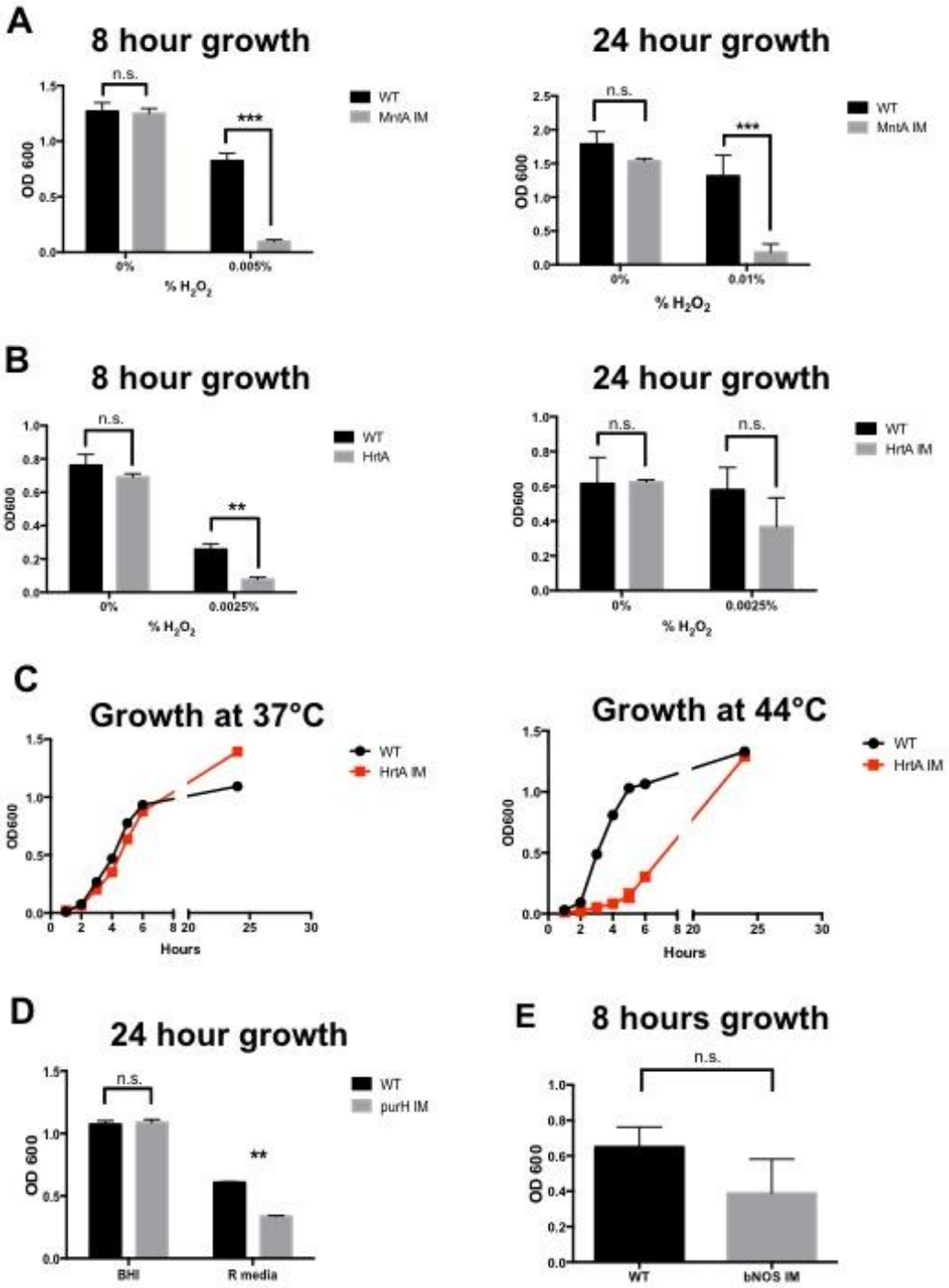

Figure 3. Re-constructed mammalian virulence mutants have an attenuated phenotype *in vitro.* A) Growth of stationary phase wild-type *B. anthracis* Sterne (WT) and *MntA IM* in hydrogen peroxide (H_2O_2) after 8 hours and 24 hours. B) Growth of log phase WT and *HrtA* IM in H_2O_2 after 8 and 24 hours. C) Growth of WT and *HrtA IM* at 37°C and 44°C in BHI. D) Growth of WT and *purH IM* in BHI and in R-minimal media after 24 hours. E) Growth of stationary phase WT and *bNOS* IM in 0.005% H_2O_2 after 8 hours. Assays were repeated at least 3 times and are shown as mean +/- SEM. Statistical significance between WT and mutant using Student's T-test with Sidak-Bonforroni correction indicated by: *p<0.05, **p<0.01, ***p<0.001.

Verification of attenuatd virulence in known *B. anthracis* mutants in *G. mellonella* infection model

Next, I tested my chromosomal mutants to see if they were attenuated for virulence in *G. mellonella.* Larvae were divided into groups of equal weigh (Fig. 4A), each worm was injected with one bacterial strain or PBS and then *G. mellonella* survival was monitored for 72 hours. As before, minimal mortality was observed with the PBS injected control (Fig 4B-G, red line), and the wild-type had an observed mortality of ~80% (Fig. 4B-G, black line). After 72 hours of infection in *G. mellonella*, significantly attenuated virulence was observed with the *MntA IM, HrtA IM, purH IM,* and *ΔclpX* strains (Fig. 4B, D, E, G; purple, pink, blue, and green lines). *ΔyceGH* had a mean mortality rate of ~55%, although this was not statistically different than wild-type (Fig. 4C). *bNOS IM* displayed no difference in virulence and was virtually indistinguishable from the wild-type (Fig. 4F, grey line). It should be noted that as I was not able to fully confirm an *in vitro* phenotype of the *bNOS IM*, it makes interpreting the lack of an *in vivo* phenotype more difficult.

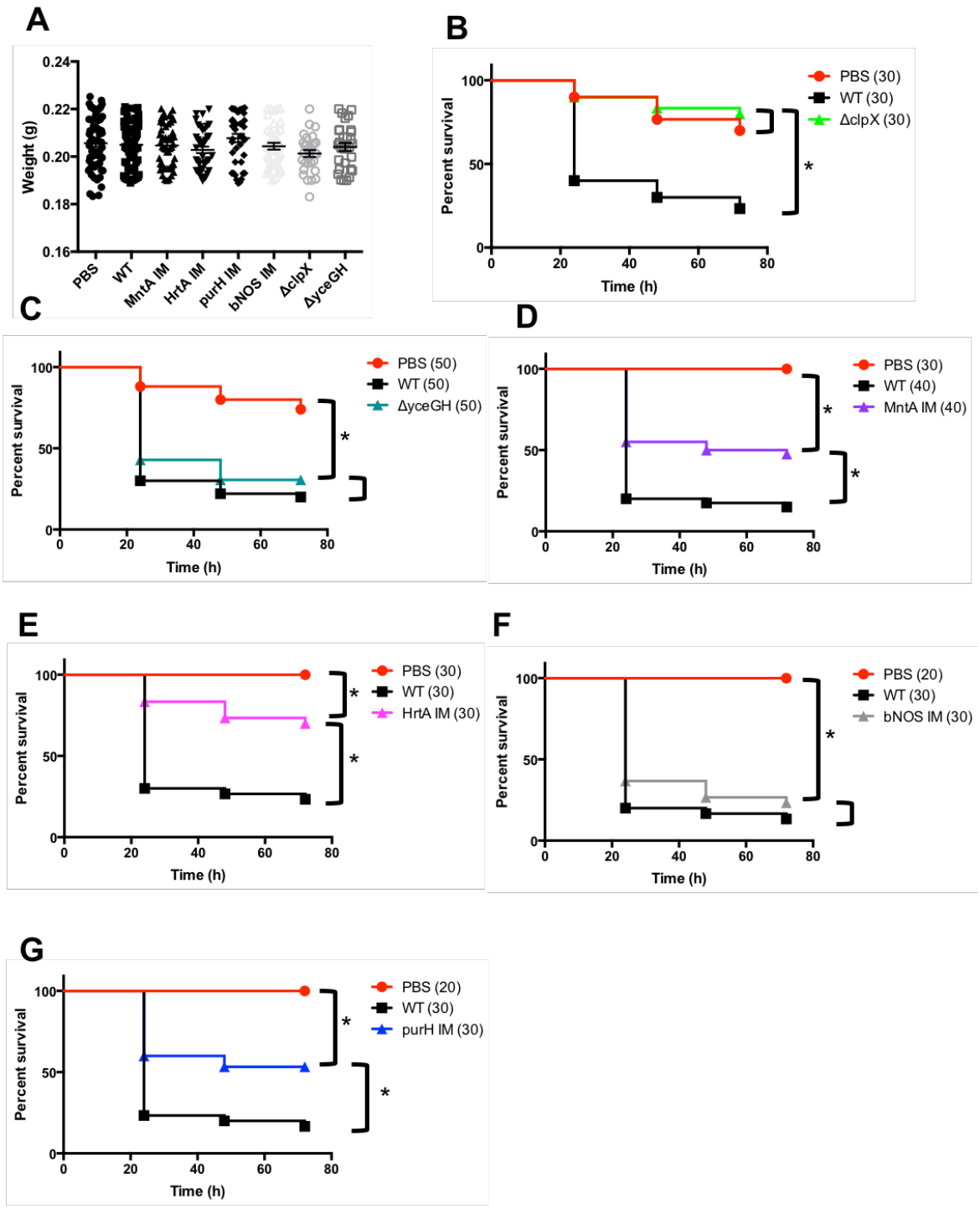

Figure 4. *B. anthracis* virulence mutants show increased survival in *G. mellonella.*
A) Larval weights for each injection group. Wild-type *B. anthracis* Sterne (WT) and saline (PBS) represent total larvae used in all trials B-G) Percent survival of larvae injected with PBS, WT, and the indicated mutants at 24, 48, and 72 hours. Each infection was repeated at least 3 independent times with 10 larvae per condition. Total number of larvae for each injection condition are indicated in parenthesis. Significance in comparison to the WT and PBS *, $p<0.025$.

Attenuation in virulence can be detected through competition assays

The virulence assays that have been described so far are survival assays, where each animal, in this case *G. mellonella*, is injected with one bacterial strain and animal survival is monitored over time. The second way to assess virulence is through a competition assay. In this assay, one worm is infected with both wild-type and mutant *B. anthracis* Sterne. This forces the mutant to directly compete with the wild-type. Theoretically if the mutant is less virulent than the wild-type, then the wild-type will proliferate more than the mutant.

In order to validate the competition assay, we tested HrtA IM and *ΔyceGH*. We reasoned that the wild-type should significantly outcompete *HrtA IM*, which had severely attenuated virulence in *G. mellonella* (Fig. 4E, pink line). The *ΔyceGH* mutant did not demonstrate a significantly attenuated *in vivo* virulence phenotype in *G. mellonella* using a survival assay, although there was a trend in that direction (~55% mortality rate *ΔyceGH* for vs. ~80% mortality rate for wild-type) (Fig. 4C). We wanted to determine whether a virulence phenotype would be seen with *ΔyceGH* in the competition assay. We grew wild-type *B. anthracis* Sterne, *HrtA IM*, and *ΔyceGH* to log phase and then combined the wild-type and either mutant in a 50/50 mixture. We then plated this 50/50 mixture on plates containing plain BHI media and plates containing antibiotic, either Erm5 for *HrtA IM* or Kan50 for *ΔyceGH*. Wild-type colonies can only grow on plain media, but the mutants contain antibiotic resistance genes. To determine mutant numbers, we simply counted the number of colonies that grew on plates containing antibiotic. To determine wild-type recovery, we counted all the colonies that grew on plain BHI and subtracted the number of colonies that grew on antibiotic media. To determine percent recovery, we took the number of wild-type or mutant colonies, divided them by the number of colonies counted on the plain BHI, and then multiplied by 100. As expected, we observed that simply mixing the two bacteria results in a 50/50 mixture (Fig. 5A, 6A). This mixture was then injected into *G.*

mellonella larvae. The infected larvae were incubated for six hours at 37°C. At this point the worms were still alive but had established infections. After 6 hours, the worms were suspended in 400ul PBS and homogenized by bead beating. The homogenate was then plated on BHI and antibiotic media. After counting colonies, we saw a significant decrease in the percent of the infection for both *HrtA IM* and *ΔyceGH* (Fig. 5C, Fig. 6C). As a control, we confirmed that bead beating itself did not lyse wild-type and the mutant at different rates (Fig. 5B, 6B). These results demonstrate that the competition method can discern virulence attenuation even with mutants such as *ΔyceGH* that are not as highly attenuated.

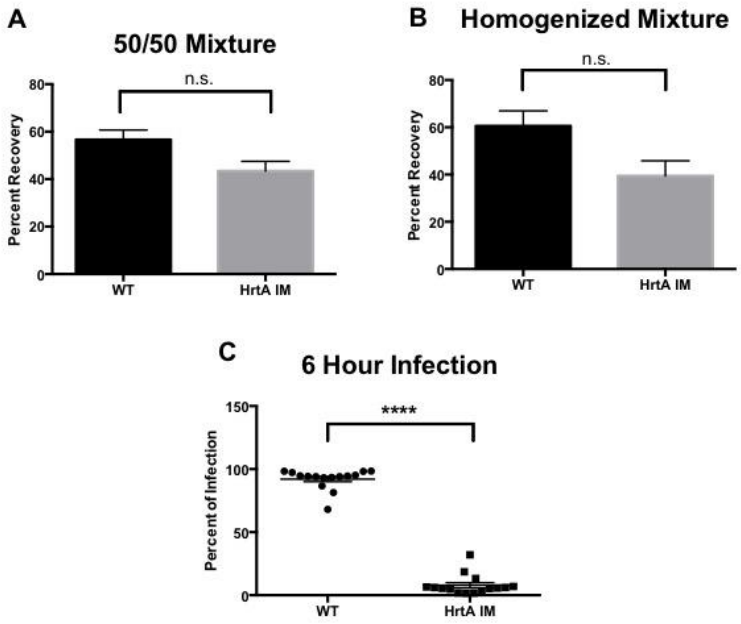

Figure 5. *HrtA IM in vivo* virulence attenuation can be identified through competition assay with wild-type. A) Recovery of wild-type and *HrtA IM* after mixing at a 1:1 ratio. B) Recovery of wild-type and *HrtA IM* after mixing at a 1:1 ratio and homogenizing. C) Percent of *B. anthracis* strain (WT or *HrtA IM*) recovered after 6 hours after injection into larvae. Assays were repeated at least 3 times and are shown as mean +/- SEM. Statistical significance between WT and mutant using Student's T-test indicated by: *p<0.05, **p<0.01, ***p<0.001.

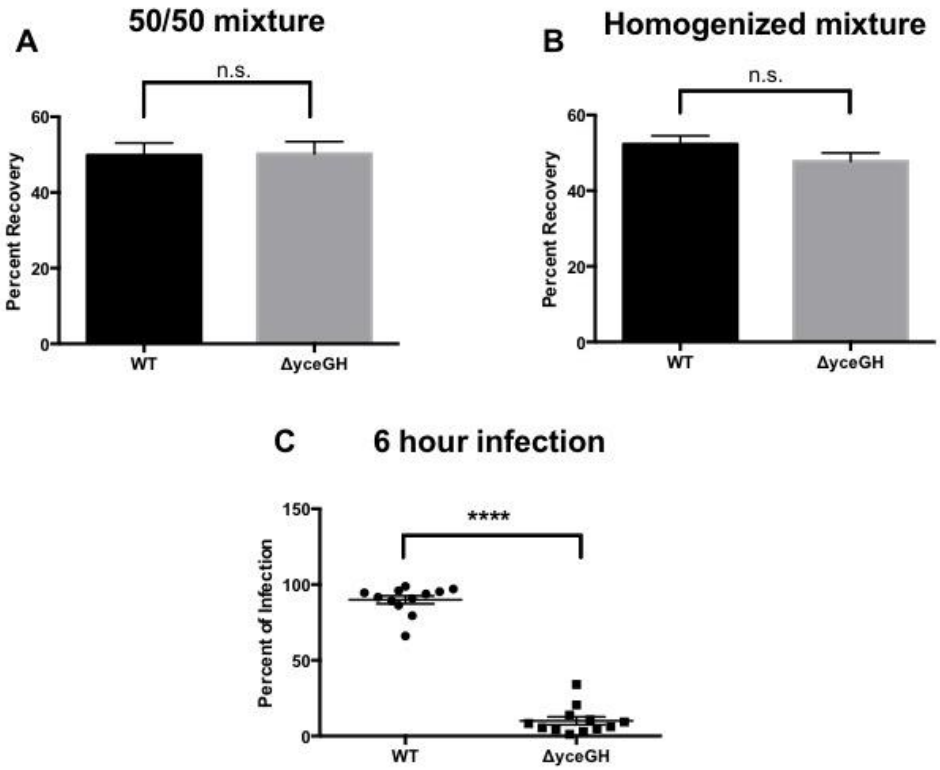

Figure 6. *ΔyceGH in vivo* virulence attenuation can be identified through competition assay with wild-type. A) Recovery of wild-type and *ΔyceGH* after mixing at a 1:1 ratio. B) Recovery of wild-type and *ΔyceGH* after mixing at a 1:1 ratio and homogenizing. C) Percent of *B. anthracis* strain (WT or *ΔyceGH*) recovered after 6 hours after injection into larvae. Assays were repeated at least 3 times and are shown as mean +/- SEM. Statistical significance between WT and mutant using Student's T-test indicated by: *p<0.05, **p<0.01, ***p<0.001.

Identification of transposon mutants with increased susceptibility to H_2O_2

After successfully completing my first objective to validate *G. mellonella* as an infection model, I next wanted to use this model to identify novel virulence genes in *B. anthracis*. However, before I could assess mutants from our transposon mutant library *in vivo*, these mutants needed to be screened *in vitro* to identify potential virulence candidates. There were three previous *in vitro* screens done in the lab that isolated mutants deficient in hemolytic or proteolytic activity as well as mutants unable to kill *C. elegans* (Franks et al., 2014; McGillivray et al., 2009). A total of 44 transposon mutants were identified by these screens. In order to narrow this number down further a previous undergraduate student, Madison Rogan, put these 44

mutants through a high-throughput H_2O_2 screen and identified 12 mutants which possessed an attenuated phenotype (Rogan, unpublished). I used a more stringent analysis, involving larger volume, shaken overnight cultures, to assess these H_2O_2 sensitive phenotypes and confirmed 6 of these 12 mutants as more susceptible to H_2O_2. These mutants, Ywle IM, 4D5, 6D10, 45F1, and 51D11, show attenuated growth in the presence of 0.01-0.02% H_2O_2 (Fig. 7A) but not in the presence of 0.12% bleach (Fig. 7B), another ROS. Therefore, despite being sensitive to H_2O_2, these transposon mutants do not exhibit sensitivity to all ROS.

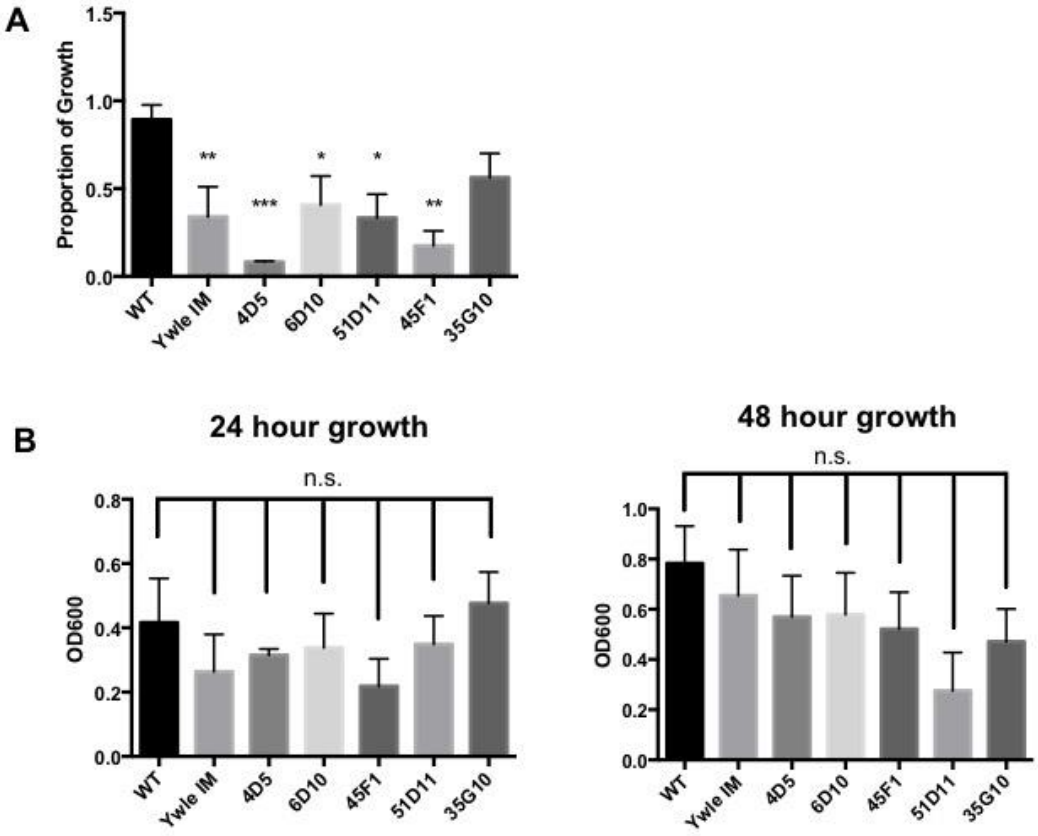

Figure 7. Transposon mutants display growth attenuation in ROS. A) Growth of overnight wild-type *B. anthracis* Sterne (WT) and indicated mutant in 0.01-0.02% H_2O_2. Proportion of growth is the optical density of the H_2O_2 exposure divided by the optical density of the unexposed culture. B) Growth of overnight wild-type *B. anthracis* Sterne (WT) and indicated mutants in 0.12% bleach after 24 and 48 hours. Assays were repeated at least 3 times and are shown as mean +/- SEM. Statistical significance between WT and mutant using one-way ANOVA and Tukey's post hoc analysis indicated by: *$p<0.05$, **$p<0.01$, ***$p<0.001$.

Because the *G. mellonella* larvae utilize ROS in their immune response, I wanted to test these ROS sensitive transposon mutants in our *G. mellonella in vivo* model. Larval weights were standardized to 190-220mg to ensure homogenous treatment groups (Fig. 8A) and each transposon mutant was injected into *G. mellonella.* After observing mortality for 72 hours, there was no attenuation in mortality for five of the six mutants (Fig. 8B). However, the 4D5 mutant did show a significant decrease in mortality (~30%) when compared to the wild-type (Fig. 8B, red line) indicating an *in vitro* and *in vivo* phenotype for one of the six transposon mutants.

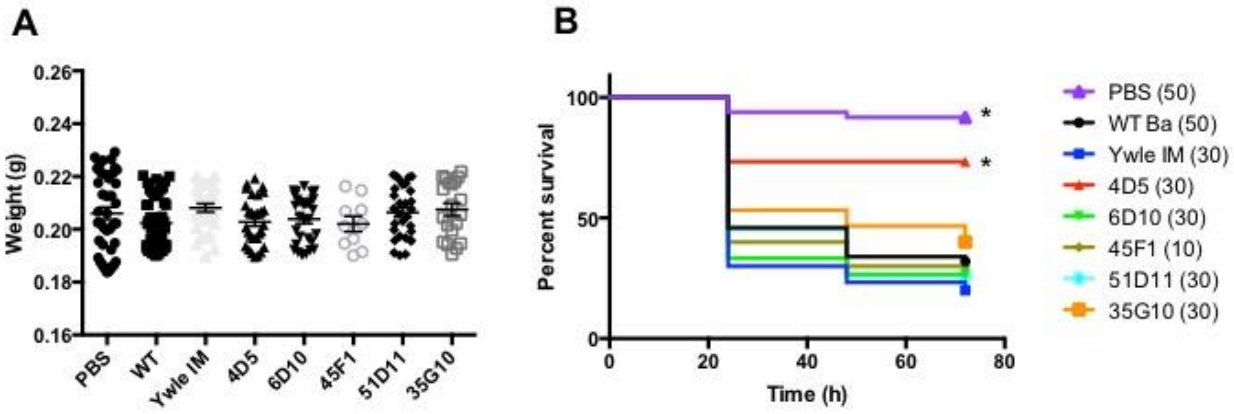

Figure 8. *G. mellonella* can identify novel ROS virulence mutants. A) Larval weights for each injection group. B) Percent survival of larvae injected with saline (PBS), wild-type *B. anthracis* Sterne (WT), and the indicated mutants at 24, 48, and 72 hours. Each infection was repeated at least 3 independent times with 10 larvae per condition. Combined results are shown. Total number of larvae for each injection condition are indicated in parenthesis. Significance in comparison to the WT *, $p<0.05$.

Identification of transposon mutants unable to acquire iron from hemoglobin

In addition to the putative H_2O_2 mutants, our lab also identified five transposon mutants that were deficient in the ability to acquire iron from hemoglobin. In this assay, *B. anthracis* strains are grown in iron-free media supplemented with hemoglobin. Wild-type *B. anthracis* Sterne is able to strip iron from the heme porphyrin ring for growth but mutants unable to acquire iron from heme will not grow. Undergraduates Julio Manceras and Mariah Green originally identified these mutants in a small screen of our transposon library, and I confirmed their phenotypes. To do this, bacteria were grown in RPMI that had all heavy metals including iron removed through chelation (cRPMI). When incubated in cRPMI, wild-type *B. anthracis* Sterne and the five transposon mutants are unable to grow (Fig. 9, middle group). When cRPMI is supplemented with hemoglobin, the wild-type grows but none of the mutants grow (Fig. 9, right group). As a control, we grew all 5 mutants in unchelated RPMI supplemented with hemoglobin to make sure the mutants did not have a general growth defect. Two of the mutants, 9D8 and 4B12, did have a phenotype just in plain RPMI, although they grew fine in BHI (data not shown). This indicates that these mutants probably have a general nutritional growth defect that may or may not be related to iron. However, growth of the other 3 mutants, 9F12, 4E12 and 22B3, was not significantly different than the wild-type in the unchelated RPMI (Fig. 9, left group).

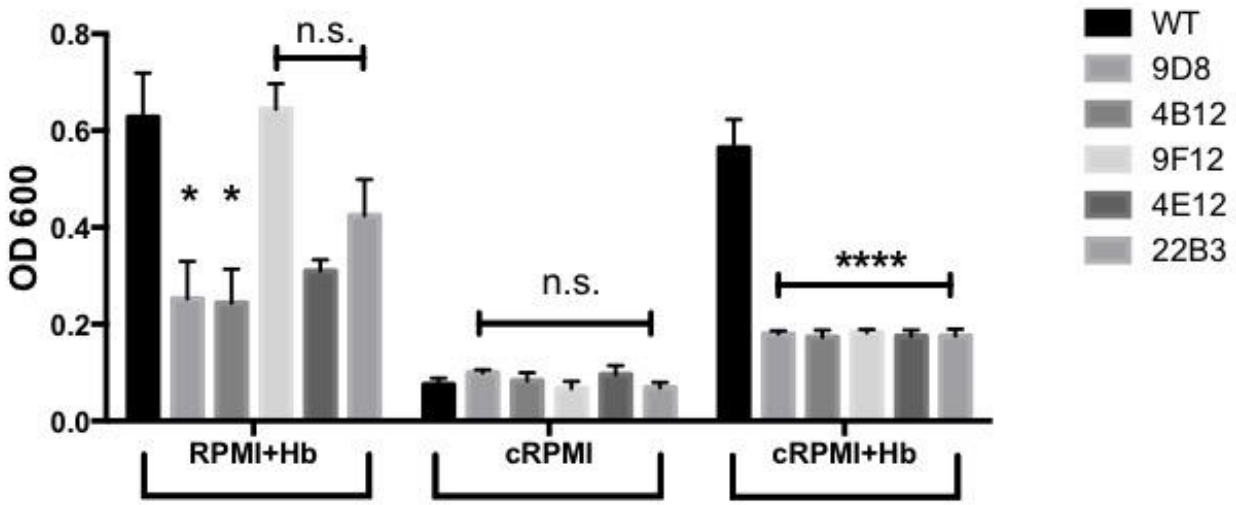

Figure 9. Iron is an essential nutrient for *B. anthracis* growth and can be acquired from hemoglobin. A) Growth of *B. anthracis* Sterne strains assessed in RPMI supplemented with hemoglobin (RPMI+Hb), chelated RPMI (cRPMI), and cRPMI supplemented with hemoglobin (cRPMI+Hb) Assays were repeated at least 3 times and are shown as mean +/- SEM. Statistical significance between WT and each mutant was determined using one-way ANOVA and Tukey's post hoc analysis indicated by: *$p<0.05$, ****$p<0.0001$.

Next, we wanted to assess these mutants in *G. mellonella.* After injecting these mutants into weight standardized larvea (Fig. 10A) and observing mortality for 72 hours, the wild-type resulted in ~80% mortality (Fig. 10B, black line) while four of the five mutants did not have any significant attenuation in mortality. However, one mutant, 9F12, demonstrated significant attenuation in virulence (~40% mortality) (Fig. 10B, purple line. Therefore, we were again able to use *G. mellonella* to identify a transposon mutant with both *in vitro* and *in vivo* virulence associated phenotypes.

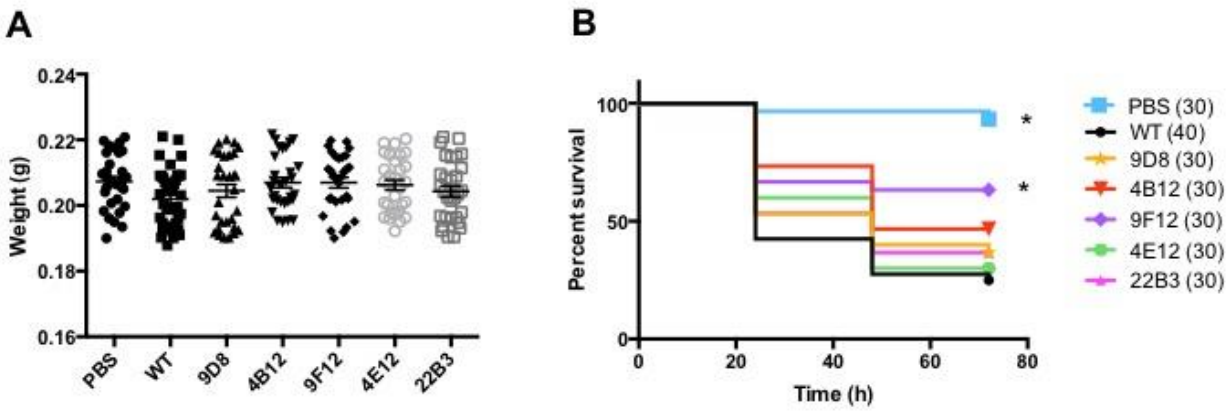

Figure 10. *G. mellonella* can identify novel iron acquisition mutants. A) Larval weights for each injection group. B) Percent survival of larvae injected with saline (PBS), wild-type *B. anthracis* Sterne (WT), and the indicated mutants at 24, 48, and 72 hours. Each infection was repeated at least 3 independent times with 10 larvae per condition. Combined results are shown. Total number of larvae for each injection condition are indicated in parenthesis. Stats description*, $p<0.05$

Site identification of transposon can be determined via Y-Linker PCR

Transposons are genetic elements that have the ability to randomly cut themselves into and out of a chromosome. Our transposon can insert itself between any adenine and thymine in the *B. anthracis* chromosomes (McGillivray et al., 2009). While we had transposon mutants, we did not know the identity of which genes were affected in many of our mutants. To discern where the transposon had inserted itself, we used the Kwon and Ricke method, which anneals a known Y-linker (Fig. 11A, orange) to the end of digested genomic DNA (Fig. 11A, green). PCR was then used to amplify the region between the transposon specific primer (Fig. 11A, yellow arrow) and a Y-linker specific primer (Fig. 11A, purple arrow). This amplified a fragment (Fig. 11A, lower panel) containing transposon (blue), genomic (green), and Y-linker sequence (orange). This amplified fragment was then sequenced and analyzed by BLAST to determine where in the *B. anthracis* genome the transposon inserted. To confirm this insertion site, another PCR was done using the same transposon specific primer (Fig. 11B, yellow) and a genomic

specific primer (Fig. 11B, navy), which was unique to a region downstream of the disrupted gene. I was able to perform and confirm this protocol for the six out of the eleven mutants, whose identity was unknown (Fig. 11C and 11D). Table 4 summarizes the function of the transposon-disrupted genes for each of the mutants used in this study.

The two transposon mutants that were attenuated for virulence in *G. mellonella*, 4D5 and 9F12, had their transposons inserted into a component of a petrobactin biosynthesis operon and a dUTPase-family gene, respectively. The 4D5 mutant's transposon was inserted into the middle of the gene; however, the 9F12 mutant had its transposon insert towards the 5' end. Interestingly, the 4E12 mutant also had its transposon inserting into the same dUTPase-family gene, just further downstream. Additionally, downstream of this dUTPase-family gene is an aminopeptidase gene which could make up an operon with the dUTPase-family gene. By using this Y-Linker method we were able to identify the location of insertion which gene was disrupted by the transposon.

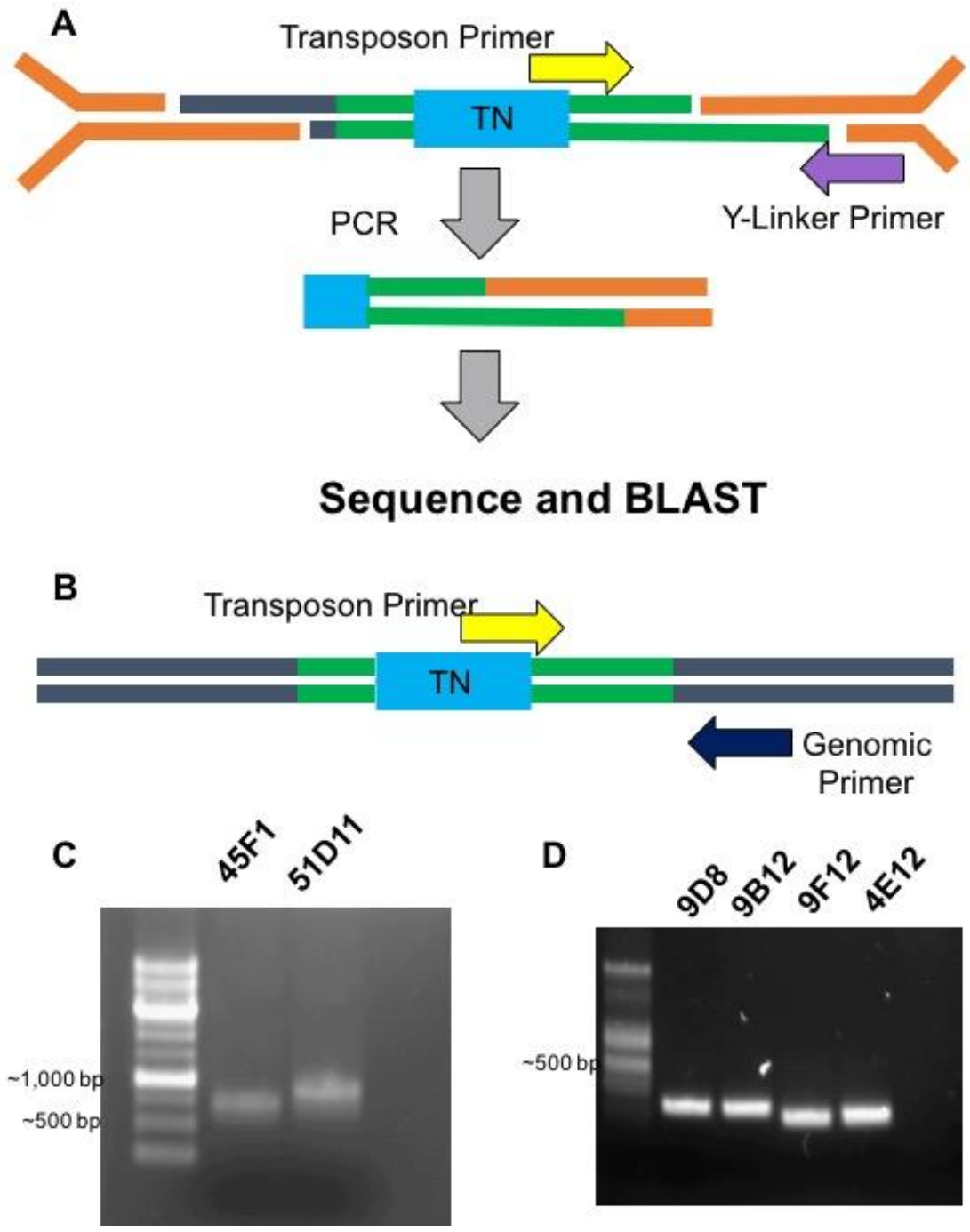

Figure 11. Identification of transposon insert. A) Y-linker (orange) annealed to digested genomic DNA (green). PCR using transposon specific primer (yellow) and Y-linker specific primer (purple) is used to amplify fragment of disrupted gene. B) Confirmation of gene disruption is done via PCR using transposon primer (yellow) and downstream genomic primer (navy). C) Gel of confirmation PCR for ROS unknown transposon mutants. D) Gel of confirmation PCR for iron acquisition mutants.

Table 4. Identity of transposon inactivated genes.

Mutant ID	Gene Identity
Ywle IM	Protein Tyrosine Kinase
4D5	Petrobactin Siderophore Biosynthesis
6D10	Sphingomyelin Phosphodiesterase
45F1/51D11	Metallobetalactamase
35G10	Glycosyl Transferase
9D8/4B12	L-Aspartate Oxidase
9F12	dUTPase Family Protein
4E12	dUTPase Family Protein
22B3	Inosine/Xanthosine Triphosphate Phosphatase

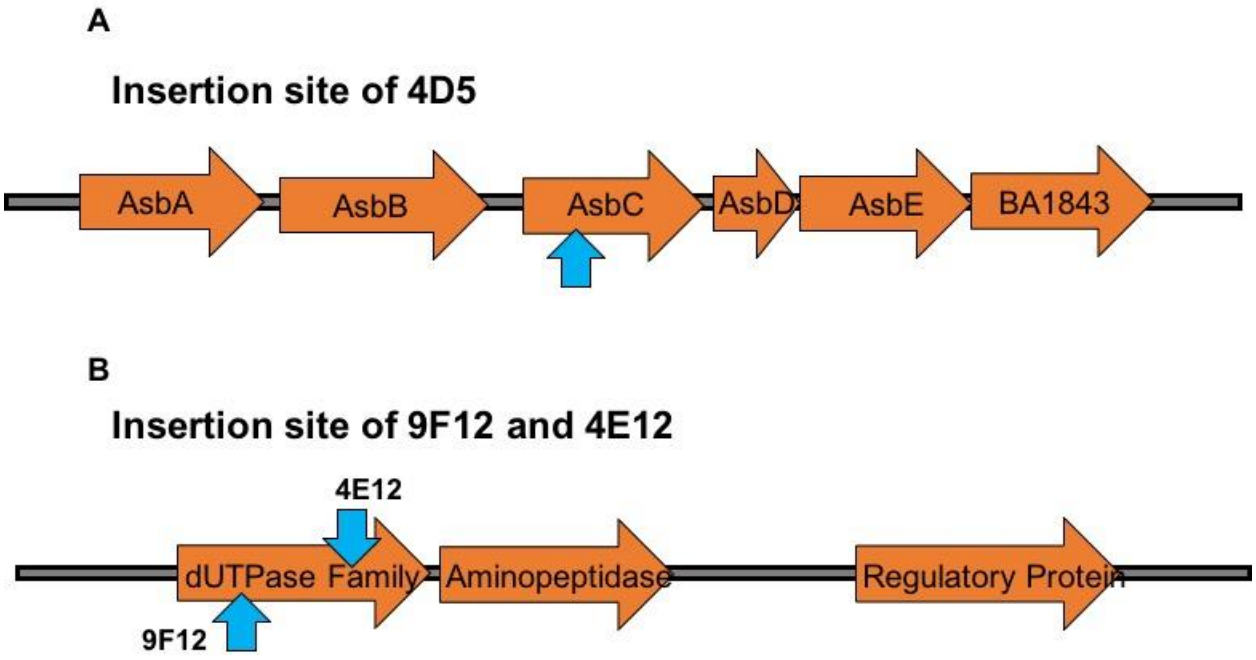

Figure 12. Schematic of transposon insertions for mutants with *in vivo* phenotype.
A) Insertion site of 4D5 indicated by arrow. B) Insertion site of 9F12 and 4E12.

DISCUSSION

Our goal was to develop the invertebrate larvae of *G. mellonella* as an alternate *in vivo* animal model for *B. anthracis.* There are multiple benefits to an invertebrate model including reduced infrastructure needs and fewer regulatory requirements. Several invertebrate infection models have been explored, and they all have advantages and disadvantages (Gravato-Nobre & Hodgkin, 2005; Kavanagh & Reeves, 2004). The downside that all invertebrates possess is their immune system is not as diverse as the vertebrate system as they lack an adaptive immune system; however, the innate immune system is highly conserved between invertebrate and vertebrate models. Our lab had previously worked with *C. elegans* as a potential invertebrate infection model, but several problems existed including that *C. elegans,* does not lend itself well to bacterial infection studies. This organism does not survive at 37°C, the optimal temperature for bacterial growth, and also requires the addition of a pore forming toxin, Cry5B, to induce pathogenicity (Gravato-Nobre & Hodgkin, 2005; Kho et al., 2011). These characteristics put significant stress on the organism, making it a highly manipulated system. Additionally, this nematode can only be exposed to bacteria orally, making it difficult to control the nematode's exposure to the bacterial pathogen (Franks et al., 2014; Gravato-Nobre & Hodgkin, 2005; Kho et al., 2011; Laaberki & Dworkin, 2008).

Because of these deficiencies, we chose to look at the insect model *G. mellonella*. Like *C. elegans*, *G. mellonella* possesses an innate immune system, but has the ability to be incubated at the necessary temperature of 37°C. This is essential because pathogenic bacteria divide most rapidly at this temperature. Additionally, this organism can be precisely inoculated through injection, and it is simple to determine larval mortality with a distinct color change from white/cream to black/brown after death (Fig. 1B). While *G. mellonella* has been used with

several fungal and bacterial pathogens (Cotter et al., 2000; Mylonakis et al., 2005; Peleg et al., 2009; Purves et al., 2010), it has yet to be validated against *B. anthracis*.

The initial step in validating this model was to show that *G. mellonella* can be incubated and injected without significant mortality. When tested, incubation showed only rare instances of mortality while injection with saline induced only ~20% mortality (Fig. 1C, green and red line). The next step in validation was to prove that the *G. mellonella* exhibits differential survival by possessing a strong enough immune system to defend against an avirulent pathogen while also succumbing to a virulent pathogen. The *ΔpX01* strain of *B. anthracis* was a good strain to determine whether *G. mellonella* can exhibit differential survival because it lacks the major virulence toxins, which are essential in causing disease. After infection, the wild-type *B. anthracis* induced ~80% mortality while the *ΔpX01* mutant demonstrated only ~20% mortality (Fig. 1), which was comparable to the saline injected control (Fig. 1C).

While *G. mellonella* met the initial requirements for an *in vivo* model for *B. anthracis* study, further validation was needed to show that the attenuation in virulence of the *ΔpX01* strain was not due to the fact that it was so severely weakened without its toxins. We also wanted to see attenuation with a variety of mutants. We chose seven previously studied virulence mutants that had already been validated in mammalian models of infection to test in our *G. mellonella* model. These seven virulence mutants had attenuated phenotypes to ROS (*ΔyceGH, MntA, HrtA, bNOS*), AMPs (*ΔclpX, ΔyceGH, mprf*), and nutritional deficits (*purH*), all of which should be detected in *G. mellonella*. Additionally, the *ΔclpX, MntA, HrtA,* and *purH* virulence genes were all initially investigated in the fully virulent strain (Ames/Vollum) of *B. anthracis*, which contains both the toxin and capsule encoding virulence plasmids pX01 and pX02. Therefore, we know that these genes play a significant role in virulence.

While two of these mutants, *ΔyceGH* and *ΔclpX,* had already been made by our lab for previous studies (Franks et al., 2014; McGillivray et al., 2009), we had to construct the remaining five mutants, *MntA IM, HrtA IM, bNOS, purH,* and *mprf* using insertional mutagenesis. After performing our mutagenesis protocol, we were unable to create the *mprf* mutant. We are unsure why we were unable to make the mutant as *mprf* is not an essential gene (Samant et al., 2009), and we had no issues creating the mutagenesis construct or getting the construct into the bacterium. Unfortunately, after temperature transitioning, insertion of the plasmid into the bacterial chromosome did not occur. However, because the *ΔclpX* mutant possesses AMP susceptibility, we did not believe that it was absolutely necessary to assess this mutant *in vivo* in order to validate our model. After construction of the remaining four mutants, we assessed each mutant for *in vitro* phenotypes consistent with the previously published phenotypes to ensure a functional mutation was created during insertional mutagenesis. Despite PCR confirmation of the *bNOS IM,* we were unable to recreate its phenotype. During the confirmation H_2O_2 assays, we observed inconsistent results with some assays showing a phenotype and others not. This resulted in a high standard error and no statistically significant difference from the wild-type *B. anthracis* Sterne.

Four of the six virulence mutants (*ΔclpX*, *MntA IM*, *HrtA IM*, *purH IM*) had a significantly attenuated virulence phenotype in *G. mellonella*. Their mortality rates ranged from ~20%(*ΔclpX*) to ~50%(*MntA* IM) while the wild-type mortality rate was ~80% (Fig. 4). These mutants were already known to be major contributors to virulence even in the fully virulent, encapsulated, strains of *B. anthracis* so these results are in line with mammalian infection models. A significant attenuation was not observed for the two remaining mutants, *ΔyceGH* and *bNOS* IM. *bNOS IM* was indistinguishable from the wild-type with ~80% mortality. However, it was difficult to interpret *bNOS IM*'s true virulence because, as mentioned earlier, we were

unable to fully confirm that we made a functional mutant. If we did not make the correct mutation, then the observation of *bNOS IM* being comparable to the wild-type would be reasonable.

The *ΔyceGH* mutant induced mortality at ~55% in comparison to 80% mortality with wild-type *B. anthracis* Sterne, although these mortality rates were not significant (Fig. 4C). Despite non-significance, this result is still similar to what was seen in mammalian models of infection where *ΔyceGH* did not demonstrate an *in vivo* mammalian survival phenotype, but did show an *in vivo* mammalian competition phenotype in previous literature (Franks et al., 2014, McGillivray unpublished data). Therefore, we developed and tested a competition assay for *G. mellonella* where we pitted the *ΔyceGH* mutant against the wild-type and saw a significant virulence phenotype (Fig. 6). The *yceGH* genes are likely not as strong a virulence determinant, which is why the phenotype of the *ΔyceGH* mutant was not evident in the survival model, but is present in the competition model. Overall, assessing previously identified virulence mutants in the *G. mellonella* invertebrate model through both survival and competition assays allowed us to prove this insect is capable of being incubated, injected without mortality, and exhibit differential survival when infected with a variety of pathogens, thus making this organism a suitable *in vivo* model.

The power of this model for our lab rests on its ability to provide a cost-effective and easy way to evaluate *in vitro* novel virulence mutants in an *in vivo* model. Because our lab does not have the capability to perform mouse infection studies, this model gives us the ability to test for an *in vivo* phenotype and serves as an additional screen to help determine which mutants we should further evaluate. Historically, our lab has utilized *in vitro* screens of a previously constructed transposon mutant library to identify novel virulence mutants (Franks et al., 2014; McGillivray et al., 2009). Some of these screens involve the use of ROS (e.g. H_2O_2) and AMP

(e.g. LL-37). These screens are consistent with the defenses of *G. mellonella's* immune system and would, therefore, allow us to assess a mutant with an interesting *in vitro* phenotype in an *in vivo* system.

To test whether *G. mellonella* can help us identify novel mutants with an *in vivo* virulence phenotype, we infected the worms with six transposon mutants that exhibited attenuated growth in H_2O_2 (Fig. 7A). We found that only one of these H_2O_2 mutants, 4D5, also demonstrated an *in vivo* survival phenotype (Fig. 8B). Based on previous studies with these six mutants, we knew the identity of the disrupted gene for these mutants (Table 4) and, therefore, knew that this mutant had its transposon inserted into the *asbC* gene, a member of a petrobactin biosynthesis operon. Petrobactin is a member of a class of compounds called siderophores, which are secreted by bacteria and scavenge the extracellular environment for iron. (Nusca et al., 2012). Iron is a crucial nutrient for many essential biochemical processes, but is cytotoxic due to the Fenton reaction which generates hydroxyl radicals (Hagan, Carlson, & Hanna, 2016; Wandersman & Delepelaire, 2004). Hydroxyl radicals are damaging to DNA and cytoplasmic membranes. Due to this destructive process, free iron is carefully regulated in biological systems with most iron bound to carrier proteins (e.g. transferrins) (Finkelstein, Sciortino, & McIntosh, 1983). Since bacteria must acquire this key element to establish an infection, siderophores strip iron away from these carrier proteins so it can be incorporated into the bacterium (Cendrowski et al., 2004). A mutation in the petrobactin biosynthesis operon has been previously described as having a virulence phenotype, however, it has not been linked with ROS sensitivity (Cendrowski et al., 2004; Nusca et al., 2012). Despite the fact that *asbC*, the site of transposon insertion for 4D5, is not a novel virulence gene, confirmation of the 4D5 virulence phenotype in an unbiased manner using *G. mellonella* further emphasizes the potential of our invertebrate model in discovering novel virulence genes. Because of the significant role of ROS in *G. mellonella,* we

would like to continue screening our transposon mutant library *in vitro* against a variety of ROS (e.g. H_2O_2, bleach, superoxide radical). If any of these screens identify attenuated *in vitro* phenotypes, we would then test them in *G. mellonella.* Based on their *in vivo* phenotypes, we could efficiently prioritize which mutants would be most interesting to follow up, potentially with a collaborator in a mammalian model.

In addition to the H_2O_2 mutants, we also tested five mutants that were unable to acquire iron from hemoglobin in *G. mellonella*. Of these five, only one, 9F12, demonstrated an *in vivo* phenotype. This mutant's transposon is inserted into a dUTPase family protein gene. This means that while this specific gene has yet to be fully characterized through unique studies, it has homology to other dUTPases in other bacterial species. Generally, dUTPases are responsible for the hydrolysis of dUTP to dUMP and pyrophosphate which is a key step in the synthesis of dTMP as well as preventing the incorporation of uracil into DNA. Directly downstream of the dUPTase gene is an aminopeptidase, which cleaves amino acids from the N-terminus of protein or peptide substrates. Based on their position in the genome, dUPTase and aminopeptidase genes are probably co-regulated as part of an operon. Therefore, the effect of the transposon insertion could be due to inhibition of the dUTPase gene, the aminopeptidase gene or both. What is interesting is that the 4E12 mutant's transposon is inserted into the same dUTPase gene as the 9F12 mutant however it is further towards the 3' end of the gene (Fig. 12B). Because these mutants disrupt the same gene, we would anticipate them displaying a similar virulence phenotype; however, while 9F12 had decreased in virulence in *G. mellonella*, 4E12 was not significantly attenuated. It is possible the catalytic component of the dUPTase protein is located at the N-terminal domain and is disrupted in the 9F12 mutant while it remains functional in the 4E12 mutant. Additionally, there could be other mutations in the 9F12 mutant and the insertion into the dUTPase gene plays no role in this iron-acquisition phenotype. The only way to ensure

this deficiency in iron acquisition is due to the dUTPase or aminopeptidase genes would be to construct independent mutations in both of these genes.

This project demonstrates that *G. mellonella* is appropriate as an *in vivo* model for *B. anthracis* Sterne. It also further confirms *G. mellonella* as an effective infection model for bacterial pathogens in general. Because this model significantly diminishes the difficulties associated with determining an *in vivo* virulence phenotype, this will be helpful to our lab in the future. It can serve as a crucial intermediate between *in vitro* virulence testing and mammalian tests and can serve as a way to prioritize future mutants that have the greatest chance of playing a significant role in virulence. *In vivo* virulence testing hinders many small-scale medical microbiology labs, so validation of a cost-effective, ethically sound model will hopefully lead to increased efficiency in studying bacterial virulence. Investigating virulence factors is important because due to the rapid rise in antibiotic resistance, there is a new idea in antibiotic development to disable pathogens by targeting and neutralizing specific toxins or virulence factors created by the infectious agent (Clatworthy et al., 2007; Palumbi, 2001). This amenable method for *in vivo* testing could help to identify undiscovered drug targets, which could aid in the development of new antibiotics or simply provide understanding of the many pathways bacteria use to cause disease.

REFERENCES

Andrews, N. C. (2000). Disorders of Iron Metabolism. *New England Journal of Medicine*, *342*(17), 1293–1294. https://doi.org/10.1056/NEJM200004273421716

Balderas, M. A., Nobles, C. L., Honsa, E. S., Alicki, E. R., & Maresso, A. W. (2012). Hal is a Bacillus anthracis heme acquisition protein. *Journal of Bacteriology*, *194*(20), 5513–5521. https://doi.org/10.1128/JB.00685-12

Bolouri Moghaddam, M. R., Tonk, M., Schreiber, C., Salzig, D., Czermak, P., Vilcinskas, A., & Rahnamaeian, M. (2016). *The potential of the Galleria mellonella innate immune system is maximized by the co-presentation of diverse antimicrobial peptides*. *Biological chemistry* (Vol. 397). https://doi.org/10.1515/hsz-2016-0157

Boman, H. G., & Hultmark, D. (1987). Cell-free immunity in insects. *Annu. Rev. Microbiol.*, *41*(103).

Cendrowski, S., MacArthur, W., & Hanna, P. (2004). Bacillus anthracis requires siderophore biosynthesis for growth in macrophages and mouse virulence. *Molecular Microbiology*, *51*(2), 407–417. https://doi.org/10.1046/j.1365-2958.2003.03861.x

Chávez, V., Mohri-Shiomi, A., & Garsin, D. A. (2009). Ce-Duox1/BLI-3 generates reactive oxygen species as a protective innate immune mechanism in Caenorhabditis elegans. *Infection and Immunity*, *77*(11), 4983–4989. https://doi.org/10.1128/IAI.00627-09

Chitlaru, T., Zaide, G., Ehrlich, S., Inbar, I., Cohen, O., & Shafferman, A. (2011). HtrA is a major virulence determinant of Bacillus anthracis. *Molecular Microbiology*, *81*(6), 1542–1559. https://doi.org/10.1111/j.1365-2958.2011.07790.x

Clarkson, J. M., & Charnley, A. K. (1996). New insights into the mechanisms of fungal pathogenesis in insects. *Trends in Microbiology*, *4*(5), 197–203. https://doi.org/10.1016/0966-842X(96)10022-6

Clatworthy, A. E., Pierson, E., & Hung, D. T. (2007). Targeting virulence: a new paradigm for antimicrobial therapy. *Nature Chemical Biology*, *3*(9), 541–548. https://doi.org/10.1038/nchembio.2007.24

Cotter, G., Doyle, S., & Kavanagh, K. (2000). Development of an insect model for the in vivo pathogenicity testing of yeasts. *FEMS Immunology and Medical Microbiology*, *27*(2), 163–169. https://doi.org/10.1016/S0928-8244(99)00185-6

Dan Dunn, J., Alvarez, L. A. J., Zhang, X., & Soldati, T. (2015). Reactive oxygen species and mitochondria: A nexus of cellular homeostasis. *Redox Biology*, *6*, 472–485. https://doi.org/10.1016/j.redox.2015.09.005

Dixon, T. C., Meselson, M., Guillemin, J., & Hanna, P. C. (1999). Anthrax. *The New England Journal of Medicine*, *341*(11), 815–826.

Doherty, C. P. (2007). Host-Pathogen Interactions : The Role of Iron 1 – 3. *The Journal of Nutrition*, *137*, 1341–1344. https://doi.org/10.3945/ajcn.113.076133.The

Fedhila, S., Buisson, C., Dussurget, O., Serror, P., Glomski, I. J., Liehl, P., … Nielsen-LeRoux, C. (2010). Comparative analysis of the virulence of invertebrate and mammalian pathogenic bacteria in the oral insect infection model Galleria mellonella. *Journal of Invertebrate Pathology*, *103*(1), 24–29. https://doi.org/https://doi.org/10.1016/j.jip.2009.09.005

Finkelstein, R., Sciortino, C., & McIntosh, M. (1983). Role of Iron in Microbe-Host Interactions. *Reviews of Infectious Diseases*, *5*, S759–S777.

Franks, S. E., Ebrahimi, C., Hollands, A., Okumura, C. Y., Aroian, R. V., Nizet, V., & McGillivray, S. M. (2014). Novel role for the yceGH tellurite resistance genes in the pathogenesis of Bacillus anthracis. *Infection and Immunity*, *82*(3), 1132–1140. https://doi.org/10.1128/IAI.01614-13

Gat, O., Mendelson, I., Chitlaru, T., Ariel, N., Altboum, Z., Levy, H., … Shafferman, A. (2005). The solute-binding component of a putative Mn(II) ABC transporter (MntA) is a novel Bacillus anthracis virulence determinant. *Molecular Microbiology*, *58*(2), 533–551. https://doi.org/10.1111/j.1365-2958.2005.04848.x

Gravato-Nobre, M. J., & Hodgkin, J. (2005). Caenorhabditis elegans as a model for innate immunity to pathogens. *Cellular Microbiology*, *7*(6), 741–751. https://doi.org/10.1111/j.1462-5822.2005.00523.x

Hagan, A. K., Carlson, P. E., & Hanna, P. C. (2016). Flying under the radar: The non-canonical biochemistry and molecular biology of petrobactin from Bacillus anthracis. *Molecular Microbiology*, *102*(2), 196–206. https://doi.org/10.1111/mmi.13465

Harris, S. H. (2002). *Factories of Death: Japanese Biological Warfare, 1932-1945, and the American Cover-up*. London: Routledge. https://doi.org/10.2307/2082105

Jenkins, A., Cote, C., Twenhafel, N., Merkel, T., Bozue, J., & Welkos, S. (2011). Role of purine biosynthesis in bacillus anthracis pathogenesis and virulence. *Infection and Immunity*, *79*(1), 153–166. https://doi.org/10.1128/IAI.00925-10

Jernigan, D. B., Raghunathan, P. L., Bell, B. P., Brechner, R., Bresnitz, E. A., Butler, J. C., … Gerberding, J. L. (2002). Investigation of bioterrorism-related anthrax, United States, 2001: Epidemiologic findings. *Emerging Infectious Diseases*, *8*(10), 1019–1028. https://doi.org/10.3201/eid0810.020353

Kato, Y., Aizawa, T., Hoshino, H., Kawano, K., Nitta, K., & Zhang, H. (2002). abf-1 and abf-2, ASABF-type antimicrobial peptide genes in Caenorhabditis elegans. *The Biochemical Journal*, *361*(Pt 2), 221–230. https://doi.org/10.1042/0264-6021:3610221

Kavanagh, K., & Reeves, E. P. (2004). Exploiting the potential of insects for in vivo pathogenicity testing of microbial pathogens. *FEMS Microbiology Reviews*, *28*(1), 101–112. https://doi.org/10.1016/j.femsre.2003.09.002

Kho, M. F., Bellier, A., Balasubramani, V., Hu, Y., Hsu, W., Nielsen-LeRoux, C., … Aroian, R. V. (2011). The pore-forming protein Cry5B elicits the pathogenicity of Bacillus sp. against Caenorhabditis elegans. *PLoS ONE*, *6*(12). https://doi.org/10.1371/journal.pone.0029122

Kwon, Y. M., & Ricke, S. C. (2000). Efficient amplification of multiple transposon-flanking sequences. *Journal of Microbiological Methods*, *41*(3), 195–199. https://doi.org/10.1016/S0167-7012(00)00159-7

Laaberki, M.-H., & Dworkin, J. (2008). Death and survival of spore-forming bacteria in the *Caenorhabditis elegans* intestine. *Symbiosis*, (46), 95–100. https://doi.org/10.1128/JB.00623-08

McGillivray, S. M., Ebrahimi, C. M., Fisher, N., Sabet, M., Zhang, D. X., Chen, Y., … Nizet, V. (2009). ClpX contributes to innate defense peptide resistance and virulence phenotypes of Bacillus anthracis. *Journal of Innate Immunity*, *1*(5), 494–506. https://doi.org/10.1159/000225955

Morton, D. B., Dunphy, G. B., & Chadwick, J. S. (1987). Reactions of hemocytes of immune and non-immune Galleriamellonella larvae to Proteusmirabilis. *Developmental & Comparative Immunology*, *11*(1), 47–55. https://doi.org/https://doi.org/10.1016/0145-305X(87)90007-3

Mylonakis, E., Moreno, R., El, J. B., Idnurm, A., Heitman, J., Stephen, B., … Calderwood, S. B. (2005). *Galleria mellonella* as a model system to study *Cryptococcus neoformans* pathogenesis. *Infection and Immunity*, *73*(7), 3842–2850. https://doi.org/10.1128/IAI.73.7.3842

Nusca, T. D., Kim, Y., Maltseva, N., Lee, J. Y., Eschenfeldt, W., Stols, L., … Sherman, D. H. (2012). Functional and structural analysis of the siderophore synthetase AsbB through reconstitution of the petrobactin biosynthetic pathway from Bacillus anthracis. *Journal of Biological Chemistry*, *287*(19), 16058–16072. https://doi.org/10.1074/jbc.M112.359349

Palumbi, S. R. (2001). Evolution - Humans as the world's greatest evolutionary force. *Science*, *293*(5536), 1786–1790. https://doi.org/10.1017/CBO9781107415324.004

Peleg, A. Y., Jara, S., Monga, D., Eliopoulos, G. M., Moellering, R. C., & Mylonakis, E. (2009). Galleria mellonella as a model system to study Acinetobacter baumannii pathogenesis and therapeutics. *Antimicrobial Agents and Chemotherapy*, *53*(6), 2605–2609. https://doi.org/10.1128/AAC.01533-08

Purves, J., Cockayne, A., Moody, P. C. E., & Morrissey, J. A. (2010). Comparison of the regulation, metabolic functions, and roles in virulence of the glyceraldehyde-3-phosphate dehydrogenase homologues gapA and gapB in Staphylococcus aureus. *Infection and Immunity*, *78*(12), 5223–5232. https://doi.org/10.1128/IAI.00762-10

Read, T. D., Peterson, S. N., Tourasse, N., Baillie, L. W., Paulsen, I. T., Nelson, K. E., … Fraser, C. M. (2003). The genome sequence of Bacillus anthracis Ames and comparison to closely related bacteria. *Nature*, *423*(6935), 81–86. https://doi.org/10.1038/nature01586

Ristroph, J. D., & Ivins, B. E. (1983). Elaboration of Bacillus anthracis Antigens in a New , Defined Culture Medium Elaboration of Bacillus anthracis Antigens in a New , Defined Culture Medium, *39*(1), 483–486.

Rogan, M. R. (n.d.). *Discovery of novel virulence mutants by assessing hydrogen peroxide sensitivity in Bacillus anthracis*.

Salzet, M. (2018). Vertebrate innate immunity resembles a mosaic of invertebrate immune responses. *Trends in Immunology*, *22*(6), 285–288. https://doi.org/10.1016/S1471-4906(01)01895-6

Samant, S., Hsu, F. F., Neyfakh, A. A., & Lee, H. (2009). The Bacillus anthracis protein MprF is required for synthesis of lysylphosphatidylglycerols and for resistance to cationic antimicrobial peptides. *Journal of Bacteriology*, *191*(4), 1311–1319. https://doi.org/10.1128/JB.01345-08

Shatalin, K., Gusarov, I., Avetissova, E., Shatalina, Y., McQuade, L. E., Lippard, S. J., & Nudler, E. (2008). Bacillus anthracis-derived nitric oxide is essential for pathogen virulence and survival in macrophages. *Proceedings of the National Academy of Sciences of the United States of America*, *105*(3), 1009–1013. https://doi.org/10.1073/pnas.0710950105

Thorne, C. B., Molnar, D. M., & Strange, R. E. (1960). Production of toxin in vitro by Bacillus anthracis and its spearation into two components. *Journal of Bacteriology*, *79*, 450–455.

Tu, W. Y., Pohl, S., Gray, J., Robinson, N. J., Harwood, C. R., & Waldron, K. J. (2012). Cellular iron distribution in Bacillus anthracis. *Journal of Bacteriology*, *194*(5), 932–940. https://doi.org/10.1128/JB.06195-11

van Sorge, N. M., Ebrahimi, C. M., McGillivray, S. M., Quach, D., Sabet, M., Guiney, D. G., & Doran, K. S. (2008). Anthrax Toxins Inhibit Neutrophil Signaling Pathways in Brain Endothelium and Contribute to the Pathogenesis of Meningitis. *PLOS ONE*, *3*(8), e2964. Retrieved from https://doi.org/10.1371/journal.pone.0002964

Vilmos, P., & Kurucz, É. (1998). Insect immunity: evolutionary roots of the mammalian innate immune system. *Immunology Letters*, *62*(2), 59–66. https://doi.org/https://doi.org/10.1016/S0165-2478(98)00023-6

Wandersman, C., & Delepelaire, P. (2004). Bacterial Iron Sources: From Siderophores to Hemophores. *Annual Review of Microbiology*, *58*(1), 611–647. https://doi.org/10.1146/annurev.micro.58.030603.123811

Watson, A., & Keir, D. (1994). Information on Which to Base Assessments of Risk from Environments Contaminated with Anthrax Spores. *Epidemiology and Infection*, *113*(3), 479–490.

VITA

Jacob Adam Malmquist was born July 23, 1993 in Honolulu, Hawaii. He is the son of Dr. Gregg and Rina Malmquist. A 2012 graduate of Bowling Green High School in Bowling Green, Kentucky, he received a Bachelor of Science degree with a major in Biology from Texas Christian University, Fort Worth, in May 2016

In August 2016, he continued his education by enrolling in graduate study at Texas Christian University, where he received his Master of Science degree in 2018. While working on his masters in Biology, he held a Teaching Assistantship and was a member of the American Society of Microbiologists. After receiving his masters, Jacob will be pursuing his Doctor of Medicine at the University of Louisville School of Medicine. Additionally, he was awarded the Army HPSP scholarship and upon completion of his medical training will be a physician in the United States Army Medical Corp.

ABSTRACT

DEVELOPMENT AND USE OF A *G. MELLONELLA* INFECTION MODEL TO DISCOVER NOVEL VIRULENCE MUTANTS IN *B. ANTHRACIS*.

By Jacob Adam Malmquist, M.S., 2018
Department of Biology
Texas Christian University

Thesis Advisor: Shauna McGillivray Ph.D., Associate Professor of Biology

Understanding bacterial virulence provides insight into the molecular basis behind infection and could identify new targets for drug development. Currently, *in vivo* virulence is assessed in the mouse model. While this model is effective, there are constraints associated with vertebrate use. This study investigated the invertebrate wax worm larvae, *G. mellonella*, as an alternative *in vivo* model for *B. anthracis*. We constructed and assessed several virulence mutants and found that *G. mellonella* effectively distinguished between virulent and avirulent strains. We also tested whether *G. mellonella* could identify novel virulence mutants. Transposon mutants were screened for deficits in reactive oxygen species (ROS) survival and iron acquisition and were then assessed in *G. mellonella*. Two were found to have an *in vivo* phenotype. These results demonstrate the potential effectiveness of *G. mellonella* as an infection model and could increase the efficiency in the identification of novel bacterial virulence mutants.